

Report 14, 1991

**GAS GEOTHERMOMETRY AND CHEMICAL EQUILIBRIA
OF FLUIDS FROM SELECTED GEOTHERMAL FIELDS**

Zhao Ping,
UNU Geothermal Training Programme,
Orkustofnun - National Energy Authority,
Grensásvegur 9,
108 Reykjavík,
ICELAND

Permanent address:
Institute of Geology,
The Chinese Academy of Sciences,
P.O. Box 634,
Beijing 100029,
P. R. CHINA

ABSTRACT

It is only relatively recently that gas chemistry has been widely used for geothermal systems. In this report, methods of collecting gas from fumaroles and wells and the chemical analysis of gas are described. Several empirical and thermodynamic gas geothermometers have been proposed in the past few years. Most of these are reviewed and evaluated mainly with data from Icelandic geothermal fields. The chemical reactions, in which gases take part in reservoirs, are discussed in detail. The WATCH aqueous speciation program is used to simulate the behaviour of minerals, which are considered to react with gas. The mineral buffer pyrite + magnetite + epidote + prehnite is suggested to control the concentration of hydrogen sulphide in a one (liquid) phase reservoir fluid. It is plausible that zoisite + prehnite + quartz + calcite control the carbon dioxide concentration in the reservoir fluid. Calculations show that carbon dioxide, hydrogen sulphide and hydrogen geothermometers are relatively efficient for Icelandic geothermal fields. Magmatic gases entering the reservoir will disturb the chemical equilibrium in the reservoir and this is reflected in the results obtained by the gas geothermometers. Condensation and separation of steam will increase the gas concentration and cause high results for gas geothermometers; the converse is true for the removal of hydrogen sulphide and hydrogen. In such cases, the co-application of different methods is more useful. The Fischer-Tropsch reaction does not seem to reach equilibrium in the fluids of most of the geothermal fields studied except in the lower zone fluid of the Krafla Leirbotnar field. Some gas geothermometers are not suited to the Icelandic geothermal fields, since their basic assumptions, such as the presence of graphite, are incorrect for these fields.

TABLE OF CONTENTS

	Page
ABSTRACT	3
TABLE OF CONTENTS	4
LIST OF FIGURES	5
LIST OF TABLES	5
1. INTRODUCTION	6
2. COLLECTION OF GAS SAMPLES AND CHEMICAL ANALYSIS	7
2.1 Sampling from wells	7
2.2 Sampling from fumaroles	8
2.3 Chemical analysis	8
3. GAS GEOTHERMOMETRY	9
3.1 Composition of steam	9
3.2 Empirical gas geothermometers	9
3.3 Thermodynamic gas geothermometers	11
3.4 Isotope geothermometers	15
3.5 Calculation of gas geothermometers from selected geothermal fields	16
4. EQUILIBRIA ASSOCIATED WITH GASES	22
4.1 Gas / gas equilibria	22
4.2 Gas / liquid equilibria - solubility	22
4.3 Mineral buffers controlling gas concentrations in geothermal reservoirs	23
5. EVALUATION AND INTERPRETATION OF RESULTS FROM SELECTED GEOHERMAL FIELDS	27
5.1 Krafla geothermal field	27
5.2 Other high-temperature fields in NE-Iceland	34
5.3 Low- and high-temperature fields in SW-Iceland	35
5.4 Kenyan geothermal fields	38
5.5 The usefulness and limitations of individual gas geothermometers	40
6. SUMMARY AND CONCLUSIONS	41
ACKNOWLEDGEMENTS	43
REFERENCES	44

LIST OF FIGURES

	Page
1. Collection of gas and steam from wells and fumaroles	7
2. Steam collected into <i>NaOH</i> solution	8
3. Temperature and steam fraction in selected wells	12
4. The locations of selected geothermal fields in Iceland	16
5. <i>FT-HSC</i> and <i>HSH-FT</i> diagrams	21
6. Gas solubility	23
7. Mineral buffers for CO_2	25
8. Mineral buffers for H_2S	26
9. The locations of the wells and fumaroles in the Krafla field	28
10. Simplified temperature profiles for the three exploited fields in the Krafla area ...	27
11. A conceptual model of the flow in the Leirbotnar and Sudurhlidar fields	27
12. Mineral equilibrium diagram for Krafla well K02	30
13. Mineral equilibrium diagrams for Krafla well K26	31
14. Mineral equilibrium diagram for Krafla well K03	32
15. Mineral equilibrium diagram for Krafla well K11	33
16. Mineral equilibrium diagram for Krafla well K14	34
17. Temperature measurements for wells BA-01 at Bakki; and H-8, G-4 and G-6 in Hveragerdi	36
18. Mineral equilibrium diagram for Bakki well BA-01	37
19. Temperature measurements for Nesjavellir wells NJ11, NJ14 and NJ16	37
20. Mineral equilibrium diagram for Hveragerði well H-8	38
21. Mineral equilibrium diagram for Hveragerði well G-4	39
22. Mineral equilibrium diagram for Hveragerði well G-6	39
23. Comparison of results of different gas geothermometers	41

LIST OF TABLES

1. Composition of steam from geothermal wells and fumaroles	17
2. Results of selected gas geothermometers	18
3. Composition of total discharge from selected wells	19
4. Temperature and steam fraction from thermodynamic methods	20
5. The chemical composition of geothermal liquid from selected fields	29
6. Comparison of temperatures obtained by solute geothermometers and those obtained using a mineral buffer	30

1. INTRODUCTION

Geochemistry is one of the most effective ways of studying geothermal reservoirs, both in the exploration and exploitation stages. Chemical composition of thermal water has proven very useful in evaluating subsurface temperature, determining water origin, observing mixing and predicting scaling and corrosion. During the last two decades, various solute geothermometers have been proposed and revised. Some of these have been extensively applied in geothermal fields with great success. Ellis (1957) pointed out that gas constituents, e.g. NH_3 and CH_4 in natural magmatic steam could be used to predict any temperature from theory. The first gas geothermometers were suggested during the nineteen seventies (Tonani, 1973). Several empirical and thermodynamic methods were subsequently proposed (D'Amore and Panichi, 1980; D'Amore et al., 1982; Arnorsson et al., 1983; Nehring and D'Amore, 1984; Arnorsson and Gunnlaugsson, 1985; D'Amore and Truesdell, 1985; Arnorsson, 1987; D'Amore et al., 1987). The application of gas chemistry to geothermal systems started relatively recently. The composition of gas and/or steam from fumaroles can be used to predict subsurface temperature, locate upflow zones and map the flow direction of boiling water. The composition of steam from discharging wells has been used to evaluate the inflow temperature, and the steam fraction, as well as boiling and multi-condensation processes. The isotopic composition of steam can be used both to identify its origin and the equilibrium temperature.

During the special training, a part of the UNU Geothermal Programme, steam sampling and analytical methods were studied. Practical work was carried out in the Hveragerdi and Krafla fields for both wells and fumaroles. Samples were analyzed at Orkustofnun (The National Energy Authority, Iceland) and at the Krafla Power Station. The different geothermometers were reviewed and tested with data mainly from Icelandic geothermal fields. The equilibrium between gases and minerals, and solvents were taken into account. The WATCH program (Arnorsson et al., 1982) is a tool for aqueous speciation and was used to simulate the behaviour in reservoirs of primary, secondary and alternative minerals, which probably control gas concentrations in the thermal fluid. The effect of magmatic activity on reservoirs, condensation and removal of H_2S , H_2 from steam during upflow was studied, and so was the change in gas composition of the fluid from a new well over the first three days of discharge.

2. COLLECTION OF GAS SAMPLES AND CHEMICAL ANALYSIS

Interpretation of the steam composition has its basis in correct sampling and analytical methods. There are some differences in the methods used for sampling wells and fumaroles (for details see Olafsson, 1988). The steam composition of well fluids was generally corrected to atmospheric pressure to get comparable values for all samples for interpretation.

2.1 Sampling from wells

The collection of representative gas samples from a discharging well involves that of dry gas (non-condensable gases), condensate, steam (in $NaOH$ solution) and hot water. It should be conducted with the aid of a Webre separator and a cooling device (Figure 1). Great care must be taken to separate steam completely from liquid. The separator is connected to the steam line and kept open to rinse and warm it up for at least 10 minutes. Then it is closed and sampling pressure (P_s) is recorded from a pressure gauge installed on the separator. The geothermal fluid is separated completely by adjusting the outlet valves. A cooling coil is connected to the steam outlet on the separator and rinsed for a few minutes before sampling. The gas and the condensate are collected in the following way. The two gas bulbs are connected by rubber tubing. A short piece of rubber tubing is connected to the second bulb and into a measuring cylinder. All the containers are rinsed with geothermal fluid from the cooling coil. When sampling, one gas bulb is first filled with condensate, then it is turned upside down and the gas made to expel the condensate into the second gas bulb and finally into the measuring cylinder. The volume of the condensate in the cylinder and the fluid temperature are recorded.

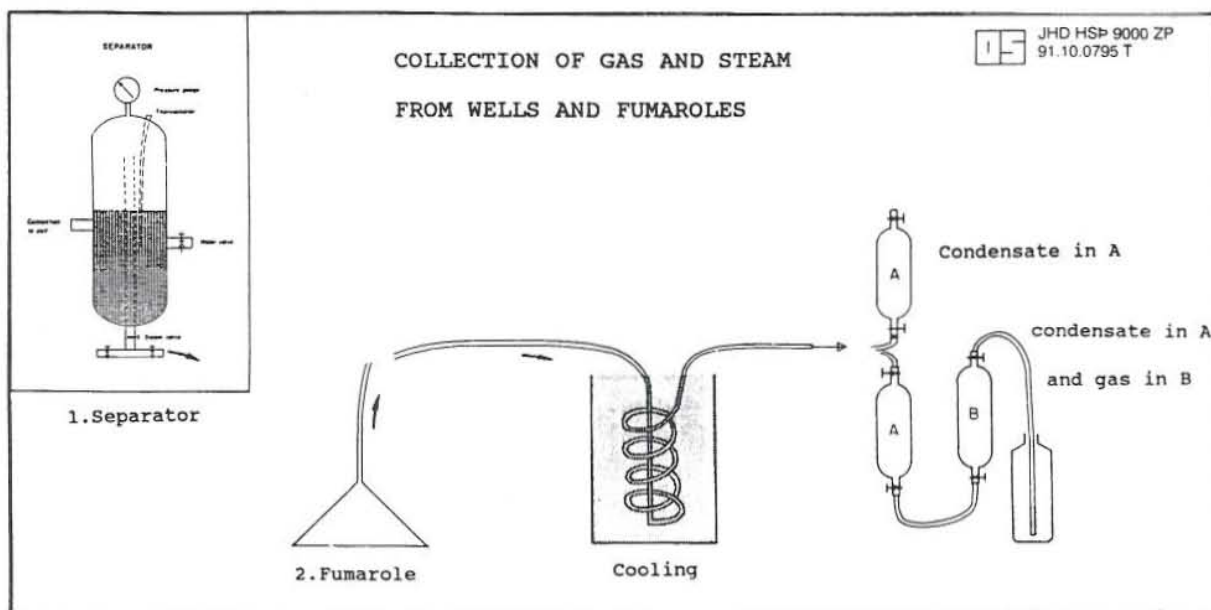


FIGURE 1: Collection of gas and steam from wells and fumaroles

Steam is collected into evacuated gas sampling bulbs containing 40% $NaOH$ solution (Figure 2). The hydroxide solution serves to dissolve quantitatively the CO_2 and H_2S from the steam. This method has the advantage that the amount of steam accompanying the gas can be determined. Finally, in order to obtain the gas concentration in the total discharge, raw untreated hot water is collected into a 250 ml glass tube for pH , CO_2 and H_2S determination.

During the training programme, three samples from wells were collected. One is from the Hveragerdi geothermal field, well H8; the others come from the Krafla geothermal field, well K26, which is a new well that had just started to discharge at the time of sampling.

2.2 Sampling from fumaroles

Before sampling, it is necessary to measure the temperature in different locations and try to find the optimum spot for sampling. A funnel is placed upside down over the major upflow and tightly packed with mud and clay to prevent atmospheric contamination. If possible, it is best to have a free flow of water from the sampling spot through the cooling device; otherwise, a vacuum pump is used. When collection begins, the containers should be rinsed thoroughly with the fluid collected. The sampling procedure is the same as for collection from a well except that no hot water is collected.

Gas samples were collected from fumaroles G5, G12 and G26 in the Krafla geothermal field and from fumarole G29 in the Hveragerdi geothermal field.

2.3 Chemical analysis

The most convenient method to determine CO_2 and H_2S is by titration, with hydrochloric acid using a pH-meter, and with mercuric acetate using dithizone as the indicator, respectively. Non-condensable gases were analyzed using gas chromatography in the chemical laboratory of Orkustofnun. The determination of pH , CO_2 and H_2S was performed on condensate and steam from fumaroles, and in addition, on hot water from wells, as soon as possible. During the Krafla field work, this was carried out in the chemical laboratory of the Krafla Power Station.

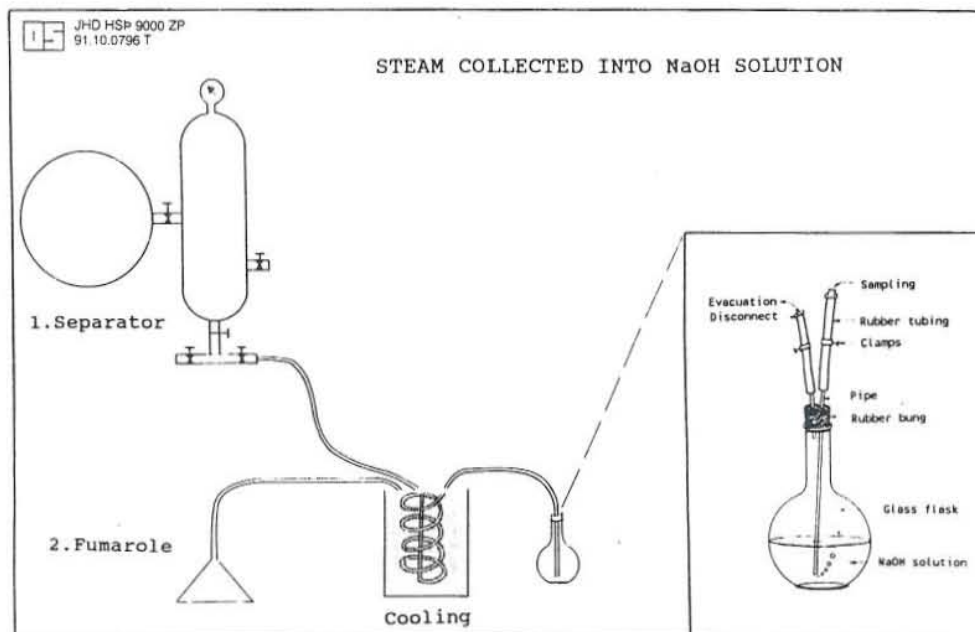


FIGURE 2: Steam collected into $NaOH$ solution

3. GAS GEOTHERMOMETRY

3.1 Composition of steam

The major gases in geothermal steam are CO_2 , H_2S , H_2 , CH_4 , N_2 , NH_3 , CO and O_2 . The noble gases in steam include He , Ne , Ar , etc. Carbon dioxide is generally the major gas component, often comprising more than 80% of the non-condensable gases and its concentration in total discharge increases with reservoir temperature. Barnes et al. (1978) found a very close correlation between CO_2 emanations and seismicity in certain areas, suggesting that the production of CO_2 is related to present tectonic activity. Kacandes and Grandstaff (1989) proposed that CO_2 in high temperature reservoirs is derived from either a deep magmatic or metamorphic source, comparing fluid composition resulting from water/rock experiments with reservoir data from several geothermal fields. In some fields, e.g. Tuscany and Larderello, Italy and Cerro Prieto, Mexico, graphite has been observed in boreholes from which it is possible to form carbon dioxide. Organic reactions in meteoric water may be a source of CO_2 in thermal fluid. The hydrogen sulphide concentration of geothermal fluids varies widely, but is thought to be formed from iron and/or silicate minerals. Hydrogen sulphide concentration commonly decreases as the steam ascends to the surface due to reactions with wallrock, dissociation to sulphur, or oxidation. The hydrogen concentration often changes with that of the hydrogen sulphide. The water dissociation is ubiquitous and of fundamental importance to all the redox processes in geothermal studies (D'Amore and Nuti, 1977). Truesdell and Nehring (1978/1979) suggested that hydrogen is produced by high temperature reaction of water with the ferrous oxides and silicates contained in reservoir rocks. Methane concentration is relatively low in steam. The Fischer-Tropsch reaction (refer to Equation 24) has been applied successfully in some geothermal fields to explain its origin (Truesdell and Nehring, 1978/1979). It also possibly derives from the decomposition of organic material and from the reaction between carbonaceous material and molecular hydrogen. Nitrogen originates from meteoric water saturated with atmospheric air, and high concentrations are found in some Krafla wells. Arnorsson (1986) attributed the latter to a volcanic source, but Armannsson et al. (1989) argued that isotopic work involving ^{15}N suggests an atmospheric origin in the Krafla field and the high nitrogen is caused by relatively low concentrations of other gases, e.g. CO_2 . Another possible origin is ammonia dissociation (D'Amore and Nuti, 1977). There is a large amount of ammonia in the Larderello field, Italy, and this is attributed to the thermal degradation of the nitrogen-rich organic material in the underlying Paleozoic-Triassic sedimentary layers (D'Amore and Nuti, 1977). The oxygen concentration is so low in uncontaminated samples that it can hardly be detected. The theoretical value is in the range of 10^{-32} to 10^{-49} bar in some reservoirs (D'Amore and Panichi, 1980).

3.2 Empirical gas geothermometers

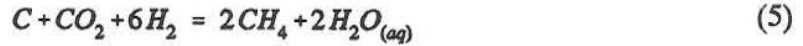
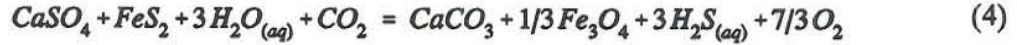
As early as in the seventies, the first empirical gas geothermometer was proposed by Tonani (1973; 1980). The relative gas concentrations were used for calculations and P_{CO_2} was assumed to be controlled by an external factor. The functions are as follows:

$$T_1(^{\circ}C) = \frac{9150}{\log \frac{CH_4}{H_2} + 1 + 16.8} - 273.15, \quad \text{for } P_{CO_2} = 0.1 \text{ atm}; \quad (1)$$

$$T_2(^{\circ}C) = \frac{9150}{\log \frac{CH_4}{H_2} + 16.8} - 273.15, \quad \text{for } P_{CO_2} = 1.0 \text{ atm} \quad (2)$$

$$T_3(^{\circ}\text{C}) = \frac{9150}{\log \frac{\text{CH}_4}{\text{H}_2} - 1 + 16.8} - 273.15, \quad \text{for } P_{\text{CO}_2} = 10 \text{ atm} \quad (3)$$

D'Amore and Panichi (1980) suggested a semi-empirical gas geothermometer based on the gas compositions of fluids from 34 thermal systems. They found that there was a relationship between the relative concentrations of H_2S , H_2 , CH_4 , CO_2 and reservoir temperatures. The following two chemical reactions were considered:



The oxygen partial pressure was assumed to be controlled by an external factor with the temperature function:

$$\log P_{\text{O}_2} = 8.20 - \frac{23643}{T(^{\circ}\text{K})} \quad (6)$$

The gas geothermometer was expressed by

$$t(^{\circ}\text{C}) = \frac{24775}{\alpha + \beta + 36.05} - 273.15 \quad (7)$$

where

$$\alpha = 2 \log \frac{\text{CH}_4}{\text{CO}_2} - 6 \log \frac{\text{H}_2}{\text{CO}_2} - 3 \log \frac{\text{H}_2\text{S}}{\text{CO}_2}, \quad (8)$$

$$\beta = -7 \log P_{\text{CO}_2} \quad (9)$$

- (a) $P_{\text{CO}_2} = 0.1$ atm if CO_2 (% by volume) < 75;
- (b) $P_{\text{CO}_2} = 1.0$ atm if CO_2 (% by volume) > 75;
- (c) $P_{\text{CO}_2} = 10$ atm if CO_2 (% by volume) > 75 and $\text{CH}_4 > 2\text{H}_2$, $\text{H}_2\text{S} > 2\text{H}_2$.

Arnorsson et al. (1983b) suggested an empirical CO_2 geothermometer, and later proposed five gas geothermometers which were calibrated with data from selected wells (Arnorsson and Gunnlaugsson, 1985). The assumption is that geothermal reservoirs are a one phase system. Three of these geothermometers are based on the total concentration of CO_2 , H_2S and H_2 in steam, respectively, and two on CO_2/H_2 and $\text{H}_2\text{S}/\text{H}_2$ ratios. Different functions for different temperatures and chlorinities were given for the H_2 , H_2S and CO_2/H_2 geothermometers, because mineralogical studies on the wells showed that different mineral buffers control gas concentrations at different temperatures for dilute water and brine reservoirs. They pointed out that it is often advantageous to calibrate geothermometers using geothermal rather than thermodynamic data, particularly when silicate mineral equilibria are involved. The error in the thermodynamic data for these minerals may produce unacceptable deviations of temperature even if the error is less than one thousandth of the enthalpy determined. The following are temperature functions for gas geothermometers:

$$T(\text{CO}_2) = -44.1 + 269.25 \log m_{\text{CO}_2} - 76.88 (\log m_{\text{CO}_2})^2 + 9.52 (\log m_{\text{CO}_2})^3 \quad (10)$$

$$T(\text{FT}) = 244.6 - 17.447Q - 0.136Q^2 - 0.0524Q^3, \quad Q = \log m_{\text{CH}_4} - \log m_{\text{CO}_2} - 4 \log m_{\text{H}_2} \quad (11)$$

$$T(\text{H}_2\text{S})^a = 246.7 + 44.81 \log m_{\text{H}_2\text{S}} \quad (12)$$

$$T(\text{H}_2)^a = 277.2 + 20.99 \log m_{\text{H}_2} \quad (13)$$

$$T(H_2S/H_2)^a = 304.1 - 39.48 \log m_{H_2S/H_2} \quad (14)$$

$$T(CO_2/H_2)^a = 341.7 - 28.57 \log m_{CO_2/H_2} \quad (15)$$

$$T(H_2S)^b = 173.2 + 65.04 \log m_{H_2S} \quad (16)$$

$$T(H_2)^b = 212.2 + 38.59 \log m_{H_2} \quad (17)$$

$$T(CO_2/H_2)^b = 311.7 - 66.72 \log m_{CO_2/H_2} \quad (18)$$

where the temperature is in °C; $T(CO_2)$ and $T(FT)$ apply to all waters;

^a: denotes valid for waters above 300°C and water in the range 200-300°C if chloride > 500 ppm;

^b: denotes valid for waters below 200°C and waters in the range 200-300°C if chloride < 500 ppm;
gas concentrations are in mmoles / kg steam.

Arnorsson (1987) developed a N_2/CO_2 gas geothermometer, which is based on the assumption that the N_2 concentration in the reservoir is derived from local meteoric water in equilibria with atmospheric air. The temperature functions for the parent reservoir water at 25°C and 5°C are given by:

$$T(N_2, 25^\circ C) = 135.9 + 63.14 Q_n + 6.241 Q_n^2 - 1.813 Q_n^3 \quad (19)$$

$$T(N_2, 5^\circ C) = 148.5 + 64.35 Q_n + 5.239 Q_n^2 - 1.832 Q_n^3 \quad (20)$$

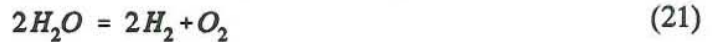
where

$$Q_n = \log(m_{CO_2}/m_{N_2}).$$

In the same paper, Arnorsson (1987) demonstrated a method for estimating partial condensation of steam during ascent of thermal fluid to the surface. The principle is that condensation in upflow results from conductive heat loss, which does not affect the N_2/CO_2 ratio in the steam. Applying this geothermometer should be discreet. The possible atmospheric contamination, both during sampling and mixing in fumaroles, may be misleading. There is also a risk that a small amount of oxygen may dissolve in a sodium or potassium hydroxide solution, thus rendering correction for such contamination difficult.

3.3 Thermodynamic gas geothermometers

The first thermodynamic gas geothermometry was developed by D'Amore et al. (1982) and was evaluated with data from the Geysers and Larderello geothermal fields. The following reactions were assumed to reach equilibria in a vapour-dominated geothermal system:



Two equations obtained are used to calculate temperature and steam fraction in reservoirs:

$$\log\left(\frac{H_2}{H_2O}\right) = -6.355 - \frac{951.6}{T} + 2.076 \log T + 1/4 \log\left(\frac{CH_4}{CO_2}\right) + \log\left(y + \frac{1-y}{B_{H_2}}\right) \quad (25)$$

$$\log\left(\frac{H_2S}{H_2O}\right) = 2.122 - \frac{2542}{T} - 0.098 \log T + 1/12 \log\left(\frac{CH_4}{CO_2}\right) + \log\left(y + \frac{1-y}{B_{H_2S}}\right) \quad (26)$$

where y is the steam fraction, and B_i is the solubility of the gas i (discussed later).

Figure 3 shows the results for samples from the Geysers field, USA and the Larderello field, Italy.

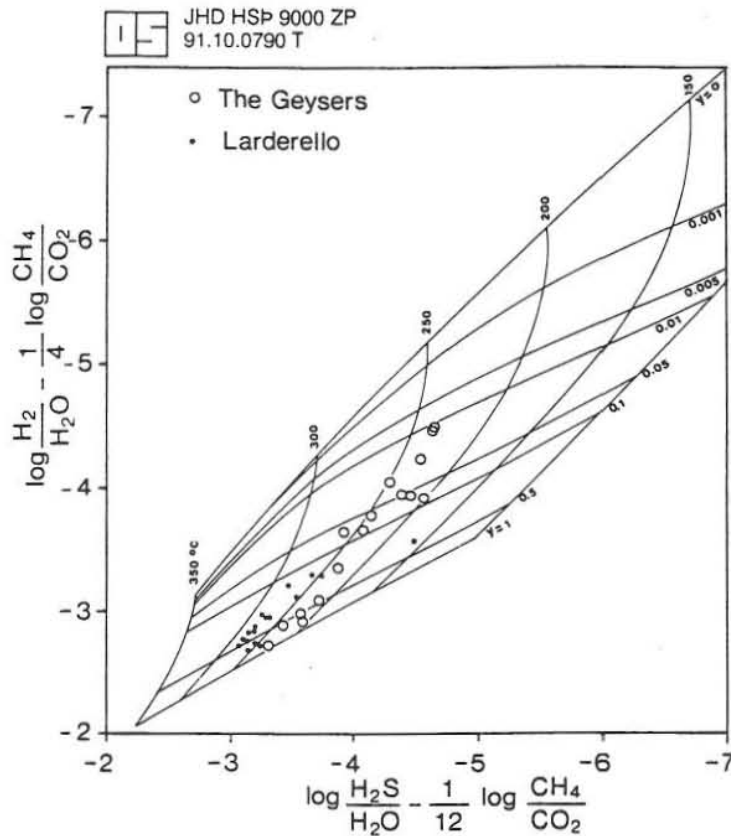


FIGURE 3: Temperature and steam fraction in selected wells

Thermodynamic gas geothermometers were developed by Nehring and D'Amore (1984). Four types of gas geothermometers were applied to gas concentrations of samples from the Cerro Prieto field, Mexico. They are based on the assumption that the fluid collected from wells is representative of the deep water in the geothermal reservoir. The following reactions between gases and minerals were considered.

(A) Fischer-Tropsch (FT):



$$\log X_{CH_4} - 4 \log X_{H_2} - \log X_{CO_2} = -21.78 + 13419/T + 4 \log Kh_{H_2} + \log Kh_{CO_2} - \log Kh_{CH_4} \quad (27)$$

(B) Hydrogen geothermometer:



$$\log X_{H_2} + 0.5 \log X_{CO_2} = 8.11 - 4501/T - \log Kh_{H_2} - 0.5 \log Kh_{CO_2} \quad (29)$$

(C) Ammonia geothermometer:



$$0.5 \log X_{N_2} + 1.5 \log X_{H_2} - \log X_{NH_3} = 5.75 - 2618/T + \log Kh_{NH_3} - 0.5 \log Kh_{N_2} - 1.5 \log Kh_{H_2} \quad (31)$$

(D) Hydrogen sulphide geothermometer:



$$\log X_{H_2S} + 1/6 \log X_{CO_2} = 10.58 - 5071.8/T - 0.79 \log T - \log Kh_{H_2S} - 1/6 \log Kh_{CO_2} \quad (33)$$

where T is in °K; X_i is the mole fraction for each gas, and Kh_i is the Henry's Law constant, respectively.

Calculations employing the above functions gave different results. The FT reaction predicted relatively high-temperatures, the H_2S reaction low temperatures and the hydrogen and ammonia reactions intermediate temperatures. The differences were attributed to different re-equilibration rates, reactions with rock and mixing with groundwater as geothermal fluid ascends to the surface.

D'Amore and Truesdell (1985) generated a new way to obtain the temperature and steam fraction in reservoirs. It is suited for both high- and low-temperature geothermal fields. The main assumptions are:

- (1) The discharge sample is obtained from a single fluid source, which consists of a two-phase mixture of liquid and vapour.
- (2) The fluid source and the reactions considered are in chemical and thermodynamic equilibria.
- (3) Neither gain nor loss of mass, nor any chemical reaction leading to re-equilibration takes place when the sample is transferred from the source to the wellhead.

The mass balance equations are built:

$$n_{H_2O,v} + n_{H_2O,l} = n_{H_2O,WH} \quad (34)$$

$$n_{i,v} + n_{i,l} = n_{i,WH} \quad (35)$$

$$B_i = (n_i/n_{H_2O})_v / (n_i/n_{H_2O})_l \quad (36)$$

$$y = n_{H_2O,v} / (n_{H_2O,v} + n_{H_2O,l}) \quad (37)$$

A_i is defined as:

$$A_i = y + (1 - y)/B_i \quad (38)$$

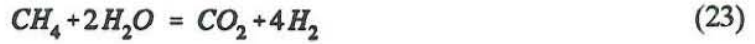
then,

$$\left(\frac{n_i}{n_{H_2O}}\right)_v = \frac{\left(\frac{n_i}{n_{H_2O}}\right)_{WH}}{A_i} \quad (39)$$

where

n_i is the number of moles of constituent i ;
subscripts v and l indicate vapour and liquid phase in reservoirs;
 WH indicates wellhead;
 y is the molar fraction of original reservoir steam with respect to total discharge;
 B_i is the molar distribution coefficient between steam and liquid phase for gas species i .

The following chemical reactions and their equilibria expressions are considered:



$$\log\left(\frac{n_{H_2}}{n_{H_2O}}\right)_{WH} = 2.652 - \frac{12776}{T} - \frac{1}{2}\log f_{O_2} + \log A_{H_2} \quad (40)$$

$$\log\left(\frac{n_{H_2S}}{n_{H_2O}}\right)_{WH} = 5.12 - \frac{6483.5}{T} - 0.79\log T - \frac{1}{6}\log f_{O_2} + \log A_{H_2S} \quad (41)$$

$$4\log\left(\frac{n_{H_2}}{n_{H_2O}}\right)_{WH} + \log\left(\frac{n_{CO_2}}{n_{CH_4}}\right)_{WH} = -25.42 - \frac{3806.6}{T} + 8.304\log T + \log\left(\frac{A_{CO_2}}{A_{CH_4}}\right) + 4\log A_{H_2} \quad (42)$$

The three equations contain three independent variables: temperature, y and oxygen fugacity. During the geothermal training programme, a computer programme was written to find the numerical solutions. D'Amore and Truesdell (1985) defined FT , HSC and HSH . The FT - HSH and FT - HSC diagrams were plotted and used to obtain graphic solutions.

$$FT = 4\log\left(\frac{H_2}{H_2O}\right) - \log\left(\frac{CH_4}{CO_2}\right) \quad (43)$$

$$HSC = 6\log\left(\frac{H_2S}{H_2O}\right) + 2\log\left(\frac{H_2}{H_2O}\right) - \log\left(\frac{CH_4}{CO_2}\right) \quad (44)$$

$$HSH = 3\log\left(\frac{H_2S}{H_2O}\right) - \log\left(\frac{H_2}{H_2O}\right) \quad (45)$$

D'Amore et al. (1987) improved the thermodynamic method by utilizing relative gas concentrations to exclude the gas/H_2O ratio, thus making it applicable for fumarole gas. The main difference is the use of the CO concentration instead of the gas/H_2O ratio. The sensitivity for CO analysis must be 0.1 ppm. The partial pressure of each gas specy in the reservoir is expressed as a function of the carbon dioxide partial pressure:

$$\log P_i = \log\left(\frac{n_i}{n_{CO_2}}\right)_d - \log A_i + \log A_{CO_2} + \log P_{CO_2} \quad (46)$$

where d is at point of discharge.

The following chemical reactions have been selected:





To eliminate S_2 and O_2 , the following equations are used to solve for T , y and carbon dioxide partial pressure:

$$4 \log\left(\frac{H_2}{CO_2}\right) - \log\left(\frac{CH_4}{CO_2}\right) = 6.69 - \frac{12144.08}{T} + 4.635 \log T + 4 \log A_{H_2} - 3 \log A_{CO_2} - \log A_{CH_4} - 4 \log P_{CO_2} \quad (49)$$

$$3 \log\left(\frac{H_2S}{CO_2}\right) - \log\left(\frac{H_2}{CO_2}\right) = 17.25 - \frac{10318.15}{T} - 0.412 \log T + 3 \log A_{H_2S} - 2 \log A_{CO_2} - \log A_{H_2} - 2 \log P_{CO_2} \quad (50)$$

$$4 \log\left(\frac{CO}{CO_2}\right) - \log\left(\frac{CH_4}{CO_2}\right) = 4.73 - \frac{12913.84}{T} + 0.719 \log T + 4 \log A_{CO} - 3 \log A_{CO_2} - \log A_{CH_4} \quad (51)$$

where the concentration of each gaseous species is expressed in moles % of dry gas sample. T is in °K. This method has been applied to selected geothermal fields in Italy and results tend to agree with measured values. It is disadvantageous that the CO concentration is usually so small that it is difficult to determine in most of the geothermal fields.

3.4 Isotope geothermometers

The isotope geothermometers are based on the isotopic fractionation between components in equilibria controlled by reservoir temperature. The difference in isotope composition between a pair of selected components can be used to evaluate the subsurface temperature. It is assumed that the isotopic composition does not change as geothermal fluid ascends to the surface. The first one was based on carbon isotope fractionation between methane and carbon dioxide and was applied in the USA. Later, various other geothermometers were proposed. Selected isotope geothermometers are listed below (T in °K) (Craig, 1975; Bottinga, 1969):

$$1000 \ln \alpha = -90.888 + 181.269 A - 8.949 A^2 \quad (52)$$

where

$$\alpha = (D/H)_{CH_4} / (D/H)_{H_2}, \quad A = 10^6 / T^2 \quad (53)$$

$$1000 \ln \alpha = -9.01 + 15.301 (10^3/T) + 2.361 (10^6/T^2) \quad (54)$$

where

$$\alpha = (^{13}C/^{12}C)_{CO_2} / (^{13}C/^{12}C)_{CH_4} \quad (55)$$

$$\ln \alpha = -0.2160 + 400.3/T + 12043/T^2 \quad (56)$$

where

$$\alpha = (D/H)_{H_2O} / (D/H)_{H_2} \quad (57)$$

$$1000 \ln \alpha = -10.55 - 9.289 (10^3/T) + 1.651 (10^6/T^2) \quad (58)$$

where

$$\alpha = \frac{(^{18}\text{O}/^{16}\text{O})_{\text{CO}_2}}{(^{18}\text{O}/^{16}\text{O})_{\text{H}_2\text{O}}} \quad (59)$$

3.5 Calculation of gas geothermometers from selected geothermal fields

The location of selected geothermal fields in Iceland are shown in Figure 4. The composition of well and fumarole steam from these low- and high-temperature geothermal fields and from three fields in Kenya is listed in Table 1 (corrected to 1 atm). In order to observe a variation in gas composition resulting from exploitation and magmatic activity, analytical results for the same fumarole or well from different times are used for the calculations. The results for different gas geothermometers are listed in Table 2, the composition of total discharge from wells in Table 3 (corrected to 1 atm) and the results of temperature and steam fraction calculations in Table 4. These are plotted in Figure 5, using the methods suggested by Nehring and D'Amore (1984) and D'Amore and Truesdell (1985).

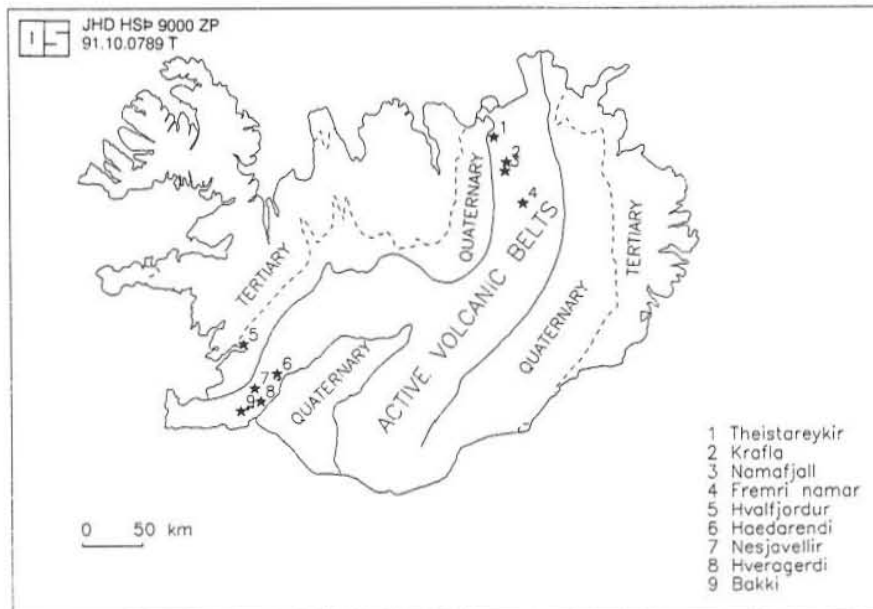


FIGURE 4: The locations of selected geothermal fields in Iceland

TABLE 1: Composition of steam from geothermal wells and fumaroles
(corrected to 1 atm, in mmoles/kg)

Location	Type	Date	CO ₂	H ₂ S	H ₂	CH ₄	N ₂	CO ₂ /H ₂ S	H ₂ S/H ₂	Source
Bakki BA-01	well	84-08-26	4.478	0.228	0.115	0.001	53.58	19.6	2.0	7
Fremri Namar a	fumarole	78-08-26	506.2	176.9	187.5	0.001	2778	2.1	0.9	8
Fremri Namar b	fumarole	84-08-26	257.3	37.42	13.58	0.220	140.9	6.9	2.8	7
Haedarendi H-2	well	83-08-03	237.7	0.144	0.012	0.024	1.053	+	12	7
Hveragerdi G-29	fumarole	91-06-06	52.85	7.249	3.468	0.167	4.371	7.3	2.1	10
Hveragerdi G-30	fumarole	86-02-21	86.91	5.723	7.954	0.337	14.72	15.2	0.7	7
Hveragerdi P-68	fumarole	85-08-08	134.2	19.43	4.684	0.097	85.31	6.9	4.2	7
Hveragerdi H-8	well	91-06-06	8.570	1.298	0.117	0.012	0.381	6.6	11	10
Hveragerdi G-4	well	80-02-13	14.39	1.401	0.306	0.049	1.473	10.3	4.6	7
Hveragerdi G-6	well	80-02-13	16.49	3.111	0.736	0.047	1.101	5.3	4.2	7
Hvalfjordur H-1	well	82-04-26	7.173	0.695	0.002	0.233	24.50	10.3	+	7
Namafjall	fumarole	86--	111.3	43.78	77.18	0.325	4.540	2.5	6.1	2
Namafjall B-11	well	90-05-28	35.31	39.88	51.51	0.166	3.382	0.9	0.8	5
Nesjavellir NJ-11	well	85-06-25	44.53	28.92	32.91	0.166	2.197	1.5	0.9	9
Nesjavellir NJ-14	well	86-06-05	36.06	6.49	0.698	0.043	1.799	5.6	9.3	9
Nesjavellir NJ-16	well	86-06-30	55.51	38.94	71.20	0.497	3.594	1.4	0.5	9
Nesjavellir N-44	fumarole	83-08-31	259.4	50.24	66.24	0.620	4.050	5.2	0.8	6
Nesjavellir N-46	fumarole	83-08-31	242.8	50.52	67.47	0.660	4.450	4.8	0.7	6
Nesjavellir N-48	fumarole	83-08-31	200.0	25.83	42.20	0.660	3.380	7.7	0.6	6
Theistareykir G-1a	fumarole	81-08-10	71.44	41.67	17.06	0.206	1.743	1.7	2.4	7
Theistareykir G-1b	fumarole	91-04-17	69.98	31.69	28.69	0.065	0.955	2.2	1.1	7
Theistareykir G-3a	fumarole	81-08-11	137.7	62.71	16.89	0.439	8.114	2.2	3.7	7
Theistareykir G-3b	fumarole	91-04-17	120.0	9.068	35.96	0.225	1.866	13	0.3	7
Theistareykir G-6a	fumarole	81-08-13	211.0	42.26	4.784	1.035	8.349	5.0	8.8	7
Theistareykir G-6b	fumarole	91-04-17	129.1	43.14	2.035	0.339	2.088	3.0	21	7
Krafla G-5a	fumarole	79-09-07	211.7	20.40	26.03	0.142	0.002	10	0.8	7
Krafla G-5b	fumarole	85-06-06	267.2	16.43	23.92	0.234	3.191	6.3	0.7	7
Krafla G-5c	fumarole	90-10-09	986.7	47.72	58.39	0.644	2.683	21	0.8	4
Krafla G-5d	fumarole	91-09-04	4805	175	310	4.346	756.8	28	0.6	10
Krafla G-6	fumarole	85-06-07	331.2	4.197	1.744	0.823	4.640	79	2.4	7
Krafla G-12a	fumarole	79-09-03	4950	112.7	36.75	1.007	0.050	44	3.1	7
Krafla G-12b	fumarole	85-06-08	2090	50.36	30.29	0.021	2.773	42	1.7	7
Krafla G-12c	fumarole	90-10-09	1407	65.97	62.17	0.019	364.2	21.3	1.1	4
Krafla G-12d	fumarole	91-09-04	1225	34.78	20.62	0.126	6.537	35.2	1.7	10
Krafla G-19a	fumarole	79-09-12	4085	29.46	28.36	2.055	0.041	+	1.0	7
Krafla G-19b	fumarole	85-06-09	392.5	21.57	23.97	0.210	2.309	18.2	0.9	7
Krafla G-19c	fumarole	90-10-08	46.51	9.361	6.832	0.078	0.001	5.0	1.4	4
Krafla G-26	fumarole	91-09-05	231.4	7.894	11.45	1.078	339.7	29.3	0.7	10
Krafla K-02	well	77-06-13	19.63	2.720	0.850	0.074	0.000	7.2	3.2	7
Krafla K-03a	well	75-11-06	19.90	5.680	5.704	0.144	0.000	3.5	1.0	7
Krafla K-03b	well	76-05-04	1868	15.87	0.019	0.019	0.019	+	+	7
Krafla K-07a	well	79-06-07	387.0	8.703	5.308	6.066	0.004	44.4	1.6	7
Krafla K-07b	well	85-06-08	56.55	9.097	2.959	0.110	0.432	6.2	3.1	7
Krafla K-10	well	77-10-26	2423	74.87	12.55	7.681	0.026	32.4	6.0	7
Krafla K-11a	well	79-06-15	464.1	6.529	0.889	0.889	0.004	71.1	7.3	7
Krafla K-11b	well	85-08-28	313.0	9.426	3.332	0.150	2.042	33.2	2.8	7
Krafla K-11c	well	90-05-23	167.1	13.57	4.828	0.158	2.833	12.3	2.8	5
Krafla K-14a	well	85-08-21	266.9	20.37	19.38	0.110	1.099	13.1	1.1	7
Krafla K-14b	well	90-05-25	259.4	26.49	26.05	0.222	4.461	9.8	1.0	5
Krafla K-20	well	90-05-22	597.3	23.50	15.73	0.216	1.708	25.4	1.5	5
Krafla K-25	well	90-11-15	136.3	26.47	4.362	0.084	1.142	5.1	6.1	7
Krafla K-26a	well	91-09-03	14.94	3.384	0.038	0.049	1.578	4.4	89	10
Krafla K-26b	well	91-09-06	38.25	3.938	0.617	0.516	11.57	9.7	6.4	10
Kenya F-13	fumarole	86-07-02	1019	0.880	6.643	15.36	0.036	+	0.1	1
Kenya F-22	fumarole	86-10-02	357.5	0.088	21.32	2.870	15.95	+	-	1
Kenya F-23	fumarole	86-10-07	9380	0.851	421.8	138.9	194.9	+	-	1
Kenya Olkaria 6	well	82-03-11	54.26	5.444	5.369	0.460	0.796	10	1.0	3

1: Armannsson (1987);

2: Muna (1982);

3: Arnorsson and Gunnlaugsson (1985);

4: Benjaminsson and Hauksson (1990);

5: Hauksson and Benjaminsson (1990);

6: Hitaveita Reykjavikur files;

7: Orkustofnun data base;

8: Oskarsson (1984);

9: Hitaveita Reykjavikur files;

10: Collected during this study;

"+" denotes ratio greater than 100;

"-" denotes ratio less than 0.1.

TABLE 2: Results of selected gas geothermometers

Location	T_D	T_1	T_2	T_3	CO_2	FT	N_2^a	N_2^b	t1	t2	t3	t4	t5	t6	t7
Bakki BA-01	235	317	358	405	101	247	77	88	218	258	296	292	131	176	206
Fremri Namar a	593	457	521	596	310	643	93	105	347	325	329	305	319	300	283
Fremri Namar b	243	298	336	379	292	392	153	166	317	301	305	287	276	256	226
Haedarendi H-2	165	232	262	295	289	176	295	305	209	237	219	262	118	136	25
Hveragerdi G-29	326	282	318	359	240	328	209	222	285	289	308	291	229	233	233
Hveragerdi G-30	227	284	320	361	258	356	187	200	281	296	312	310	222	247	242
Hveragerdi P-68	230	295	332	375	272	352	149	161	304	291	300	280	257	238	214
Hveragerdi H-8	292	271	305	344	148	229	228	241	252	258	288	263	181	176	187
Hveragerdi G-4	272	265	299	337	179	252	203	216	253	266	294	278	183	192	200
Hveragerdi G-6	312	278	313	353	187	280	216	228	269	274	303	279	205	207	222
Hvalfjordur H-1	108	185	209	236	136	12	104	116	240	218	237	199	163	103	66
Namafjall	474	320	361	408	267	460	231	243	320	317	337	314	280	285	301
Namafjall B-11	392	325	366	414	224	434	205	218	318	313	346	308	277	278	323
Nesjavellir NJ-11	353	317	358	404	234	415	225	237	312	309	338	306	268	271	303
Nesjavellir NJ-14	225	278	314	354	225	286	225	237	283	274	293	266	226	206	197
Nesjavellir NJ-16	366	312	352	397	242	441	217	229	318	316	345	314	277	284	319
Nesjavellir N-44	406	307	346	391	292	455	260	271	323	315	325	309	284	282	272
Nesjavellir N-46	409	306	345	390	290	454	255	266	323	316	326	309	284	283	275
Nesjavellir N-48	382	299	337	380	284	428	257	269	310	311	322	312	265	275	267
Theistareykir G-1a	297	303	342	386	251	389	246	258	319	303	324	289	279	260	270
Theistareykir G-1b	332	331	373	422	251	425	264	275	314	308	331	302	271	268	286
Theistareykir G-3a	274	291	328	371	273	388	220	232	327	303	316	282	290	260	251
Theistareykir G-3b	311	314	354	400	269	427	260	271	290	310	327	328	235	272	277
Theistareykir G-6a	403	261	294	331	286	336	232	244	320	291	295	267	279	238	202
Theistareykir G-6b	404	264	298	336	271	312	259	270	320	284	290	252	280	224	191
Krafla G-5a	365	316	356	403	286	424	381	373	305	307	316	308	258	267	251
Krafla G-5b	338	306	346	390	293	417	268	279	301	306	312	311	252	265	242
Krafla G-5c	332	304	343	388	328	466	308	317	322	314	307	308	282	280	230
Krafla G-5d	322	301	339	383	380	564	190	203	347	330	308	314	319	308	232
Krafla G-6	208	251	282	318	299	308	263	274	275	282	277	289	214	222	160
Krafla G-12a	251	290	327	370	381	456	381	372	339	310	281	285	307	273	170
Krafla G-12b	314	352	397	450	351	487	326	333	323	308	289	295	284	269	189
Krafla G-12c	273	368	416	472	339	527	175	188	328	315	303	303	292	281	221
Krafla G-12d	294	314	354	400	335	436	290	300	316	305	291	295	273	263	193
Krafla G-19a	228	276	311	351	374	432	381	372	313	308	280	303	269	268	168
Krafla G-19b	328	308	348	393	303	423	288	298	306	306	307	306	260	265	231
Krafla G-19c	287	304	343	387	235	358	381	373	290	295	318	299	236	244	256
Krafla G-26	223	272	307	346	289	368	126	138	287	299	304	310	232	253	224
Krafla K-02	317	273	308	348	196	281	378	367	266	276	303	284	202	209	220
Krafla K-03a	288	292	329	371	197	338	382	374	281	293	326	304	222	241	275
Krafla K-03b	175	241	272	306	347	210	381	372	300	241	199	188	251	146	-22
Krafla K-07a	235	239	270	304	303	329	381	372	289	292	288	296	234	240	187
Krafla K-07b	330	286	322	364	243	327	280	291	290	287	305	285	236	230	226
Krafla K-10	313	247	278	314	356	376	381	372	331	300	276	273	295	255	159
Krafla K-11a	270	241	271	305	308	288	381	372	283	276	264	270	226	210	130
Krafla K-11b	362	283	319	360	297	343	285	295	290	288	285	286	237	232	180
Krafla K-11c	308	288	324	366	279	350	257	269	297	292	298	286	247	239	209
Krafla K-14a	353	315	356	402	293	416	297	307	305	304	309	303	258	262	236
Krafla K-14b	349	309	348	393	292	421	257	268	310	307	313	304	266	267	245
Krafla K-20	303	301	339	383	315	408	307	316	308	302	297	297	262	258	206
Krafla K-25	451	296	333	377	273	351	278	288	310	291	299	273	266	237	212
Krafla K-26a	187	238	268	302	181	185	202	215	270	247	267	227	208	157	138
Krafla K-26b	194	243	274	309	227	263	170	183	273	273	291	272	212	204	192
Kenya F-13	139	231	260	293	329	337	381	377	244	294	279	339	170	244	166
Kenya F-22	140	267	301	340	301	388	228	240	199	305	307	398	105	263	230
Kenya F-23	175	255	288	324	409	537	251	263	244	332	303	411	169	314	222
Kenya Olkaria 6	244	274	308	348	241	335	261	273	280	293	313	304	221	240	245

T_D : calculated from D'Amore and Panichi (1980);

T_1, T_2, T_3 : calculated from Tonani (1973; 1980), refer to the partial pressure of carbon dioxide 0.1 atm, 1.0 atm, 10 atm, respectively;

CO_2, FT : calculated from Arnorsson (1985);

N_2^a, N_2^b : calculated from Arnorsson (1987), refer to 25°C and 5°C (see text for detail);

t1, t2, t3, t4: calculated from Arnorsson and Gunnlaugsson (1985), refer to $H_2S, H_2, CO_2/H_2$ and H_2S/H_2 gas geothermometers (see Equations 12, 13, 14 and 15);

t5, t6, t7: calculated from Arnorsson and Gunnlaugsson (1985), refer to H_2S, H_2 and CO_2/H_2 gas geothermometers (see Equations 16, 17 and 18).

TABLE 3: Composition of total discharge from selected wells
(corrected to 1 atm, in mmoles/kg)

Location	Ps	Enthalpy	CO ₂	H ₂ S	H ₂	CH ₄
Bakki BA-01	0.8	572 ^c	0.470	0.020	0.008	0.0004
Hveragerdi H-8	6.2	772 ^c	2.636	0.720	0.018	0.002
Hveragerdi G-4	5.7	780 ^c	3.490	0.812	0.049	0.008
Hveragerdi G-6	5.5	1602 ^m	5.319	1.370	0.210	0.013
Namafjall B-11	7.4	2066 ^m	26.14	30.10	37.60	0.121
Nesjavellir 11	8.4	2251 ^m	36.26	24.24	26.72	0.135
Nesjavellir 14	6.5	1236 ^c	16.40	3.364	0.310	0.019
Nesjavellir 16	12.5	2123 ^m	42.08	30.34	53.78	0.376
Krafla K-02	4.2	821 ^c	5.361	1.509	0.152	0.013
Krafla K-03 ^a	8.4	1083 ^m	7.208	3.177	1.681	0.042
Krafla K-03 ^b	1.7	1053 ^m	530.3	4.681	0.005	0.005
Krafla K-07 ^a	2.9	1636 ^m	210.7	4.950	2.864	3.274
Krafla K-07 ^b	2.1	1452 ^m	27.18	4.837	1.356	0.050
Krafla K-10	20	1341 ^m	995.5	31.79	5.130	3.142
Krafla K-11 ^a	6.5	1903 ^m	307.7	4.545	0.585	0.585
Krafla K-11 ^b	12.5	1658 ^m	174.4	5.664	1.831	0.082
Krafla K-11 ^c	3.5	2037 ^m	120.8	10.07	3.463	0.114
Krafla K-14 ^a	11.6	2626 ^m	261.3	20.07	18.95	0.108
Krafla K-14 ^b	6.8	2654 ^m	257.4	26.33	25.80	0.220
Krafla K-20	5.0	2145 ^m	461.3	18.21	12.04	0.165
Krafla K-25	22.5	1741 ^m	80.72	16.10	2.557	0.049
Krafla K-26 ^a	2.3	795 ^c	3.63	1.15	0.006	0.008
Krafla K-26 ^b	2.7	850 ^c	8.491	1.50	0.118	0.099
Kenya Olkaria-6	4.8	2281 ^m	45.03	4.514	4.431	0.380

Ps: sampling pressure (bar g);
^m: water flow and critical lip pressure measurement (kJ/kg);
^c: inflow temperature measured (kJ/kg).

TABLE 4: Temperature and steam fraction from thermodynamic methods

Location	T _{in} (°C)	FT ¹⁾	CO ₂ /H ₂ ¹⁾	CO ₂ /H ₂ S ¹⁾	FT-HSC ²⁾	Y ²⁾
Bakki BA-01	136	282	211	207	171	0.0008
Hveragerdi H-8	182	266	217	244	----	----
Hveragerdi G-4	184	286	238	248	----	----
Hveragerdi G-6	216	312	255	266	259	0.001
Namafjall B-11	320	452	351	335	248	0.90
Nesjavellir 11	325	437	344	327	256	0.612
Nesjavellir 14	278	317	261	287	----	----
Nesjavellir 16	326	458	364	337	----	----
Krafla K-02	193	315	259	264	----	----
Krafla K-03 ^a	245	369	297	281	267	0.024
Krafla K-03 ^b	245	251	231	328	----	----
Krafla K-07 ^a	280	361	327	304	276	0.03
Krafla K-07 ^b	260	359	294	297	284	0.018
Krafla K-10	290	403	368	376	336	0.015
Krafla K-11 ^a	290	321	291	298	288	0.0015
Krafla K-11 ^b	290	374	315	305	286	0.04
Krafla K-11 ^c	290	381	316	312	298	0.06
Krafla K-14 ^a	275	438	352	326	235	0.97
Krafla K-14 ^b	275	442	359	333	244	0.99
Krafla K-20	290	431	357	334	267	0.43
Krafla K-25	270	381	311	330	320	0.022
Krafla K-26 ^a	190	232	202	268	----	----
Krafla K-26 ^b	195	296	259	275	----	----
Kenya Olkaria-6	242	366	306	284	258	0.077

- 1) Geothermometer of Nehring and D'Amore (1984);
2) Geothermometer of D'Amore and Truesdell (1985);
T_{in}: main inflow temperature;
"----" denotes no solution obtained.

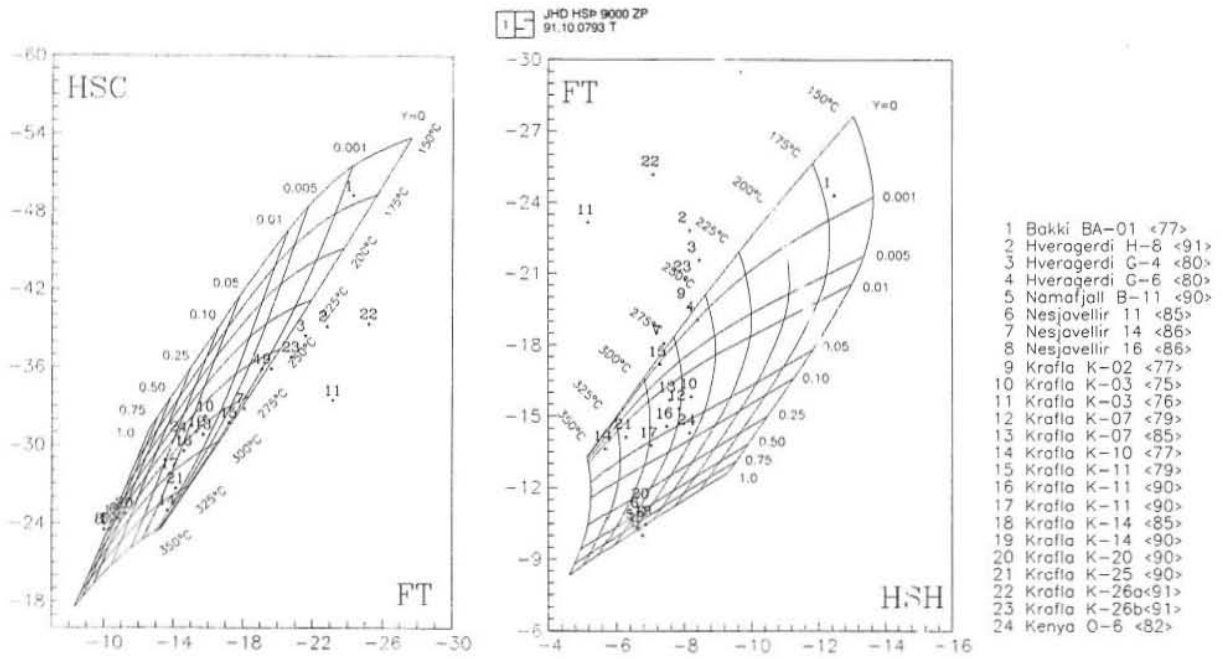


FIGURE 5: A) FT-HSC diagram; B) HSH-FT diagram

4. EQUILIBRIA ASSOCIATED WITH GASES

4.1 Gas / gas equilibria

In geothermal systems, the possible reactions between gases are described by the Fischer-Tropsch reaction, the dissociation of H_2O , H_2S and NH_3 (gas reaction with minerals is not discussed in this section):



Giggenbach (1980) concluded that the first two reactions are close to equilibrium in the fluids of some geothermal fields, such as Wairakei, Broadlands and Kawerau, New Zealand and assumed that the gas composition of total discharge represented the gas composition in the reservoirs. The thermodynamic geothermometry suggested by D'Amore et al., 1982; Nehring and D'Amore, 1984 and D'Amore and Truesdell, 1985, 1988, is also based on the Fischer-Tropsch reaction, which is assumed to approach equilibrium in reservoirs. Arnorsson and Gunnlaugsson (1985) argued on the basis of the data from selected geothermal fields that the concentrations of CO_2 , CH_4 and H_2 were not in equilibrium, and that the composition of total discharge does not accurately reflect the composition of inflow into reservoirs. The deviation would depend on the extent of boiling processing. Geothermometer temperatures based on the Fischer-Tropsch reaction are commonly much higher than measured ones. It should be pointed out that this reaction needs a long time or a high temperature to reach equilibrium. Another possible gas reaction is oxidation of CH_4 , like H_2 and H_2S , by oxygen dissolved in groundwater following mixing during the ascent of the geothermal fluid to the surface.

4.2 Gas / liquid equilibria - solubility

A thermodynamic equilibrium exists for the distribution of gases between vapour phase and liquid phase in reservoirs. The behaviour of gases is described by Henry's Law:

$$P_i = Kh_i X_i \quad (60)$$

where

P_i is the partial pressure of a gas i in the vapour phase;

X_i is its molar fraction in the liquid phase;

Kh_i is the Henry's Law constant, which can be measured experimentally.

Giggenbach (1980) and D'Amore et al. (1982) adopted the gas distribution coefficient B_i (defined in Chapter 3.3) instead of the Henry's Law constants. The conversion from Kh_i to B_i is represented by:

$$B_i = Kh_i V_i / (RT) \quad (61)$$

where

R is the gas constant;

V_i is the specific volume of steam;

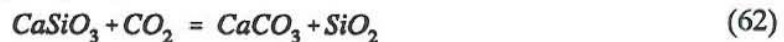
T is the temperature in °K.

The B_i values from Giggenbach (1980) and D'Amore and Truesdell (1988) are shown in Figure 6. It is clear that NH_3 is the most soluble in water, and N_2 the least soluble. There is no difference between the two sets of data except that the hydrogen solubility of D'Amore and Truesdell (1988) is slightly lower than that of Giggenbach (1980).

4.3 Mineral buffers controlling gas concentrations in geothermal reservoirs

The chemical composition of geothermal fluids is generally dependent on rock type, recharge water, temperature and pressure in the reservoirs. Some geothermal fields are affected by volcanic activity. Magmatic fluid enters reservoirs and influences the composition of original geothermal fluid, such as happened in the Krafla field, Iceland in the 1970's and early 1980's. Various physical processes and chemical reactions take place in geothermal systems. Thermodynamic equilibrium for the distribution of gases between vapour and liquid phase are reached faster than other equilibria. Isotopic equilibria seem to need a relatively long time, especially in the case of the Fischer-Tropsch reaction. Only few chemical reactions predominate and possibly reach equilibrium. The primary, secondary and alteration minerals affect the composition of geothermal fluids, gases and solutes.

Giggenbach (1981) found that pyrite + iron containing aluminum silicates are the mineral assemblages that are expected to control the H_2S/H_2 ratios. The carbon dioxide fugacities in New Zealand geothermal fields are fixed by the mineral buffers, plagioclase, clay and calcite (Giggenbach, 1981). Oskarsson (1984) expected the



reaction to control the CO_2 when the magmatic gas is added to geothermal fluids. Nehring and D'Amore (1984) proposed that pyrite + magnetite affected the H_2S/H_2 ratio and graphite + water affected CO_2 and H_2 partial pressure in the Cerro Prieto field, Mexico. Arnorsson and Gunnlaugsson (1985) observed that the mineral assemblage epidote + prehnite + calcite + quartz governs the CO_2 concentration in reservoirs at temperatures above 200°C and another mineral buffer zeolite + calcite may dominate at lower temperatures. Two different buffers are

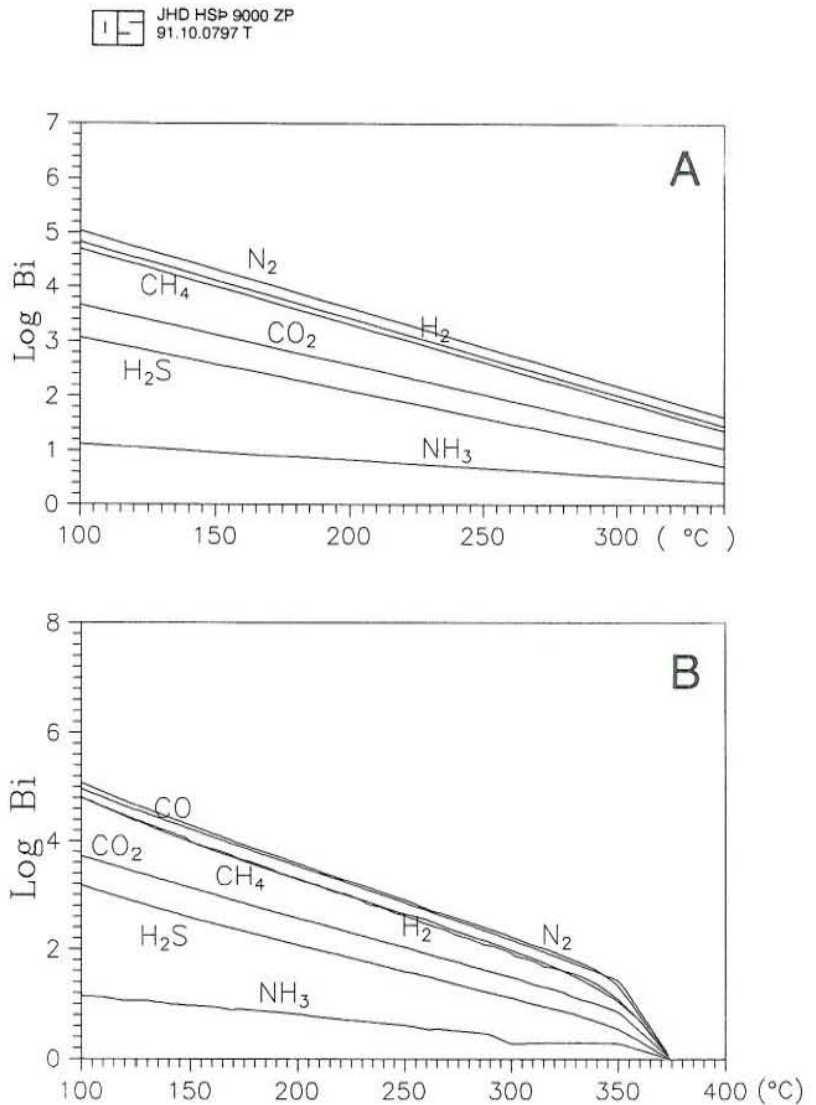


FIGURE 6: Gas solubility based on
A) Giggenbach, 1980; B) D'Amore and Truesdell, 1988

in equilibrium with H_2S and H_2 . The pyrite + pyrrhotite + epidote + prehnite buffer dominates in dilute water but the pyrite + epidote + prehnite + chlorite buffer or magnetite in brine. The several potential mineral buffers that control CO_2 , and H_2S are discussed below.

At a given pressure and temperature, the free energy of formation of a pure phase from the elements, $\Delta G^{P,T}$, is defined by

$$\Delta G^{P,T} = \Delta H^{P,T} - TS^{P,T} \quad (63)$$

where

$$\Delta H^{P,T} = \Delta H_f^{P_r, T_r} + \int_{T_r}^T C_p dT + \int_{P_r}^P \{V^{P_r, T_r} - T \left(\frac{\delta V}{\delta T}\right)_P\} dP \quad (64)$$

$$S^{P,T} = S^{P_r, T_r} + \int_{T_r}^T \left(\frac{C_p}{T}\right) dT - \int_{P_r}^P \left(\frac{\delta V}{\delta T}\right)_P dP \quad (65)$$

$\Delta H_f^{P_r, T_r}$ is the apparent enthalpy of formation of the pure phase from the elements at the reference temperature 298.15°K and the pressure 1 bar;
 S^{P_r, T_r} , V^{P_r, T_r} and C_p are the enthalpy, molar volume and heat capacity at constant pressure, respectively.

The two expressions selected for the calculation of C_p are (Helgeson, 1969; Berman, 1988):

$$C_p = a + bT - cT^{-2} \quad (66)$$

$$C_p = k_0 + k_1 T^{-0.5} + k_2 T^{-2} + k_3 T^{-3} \quad (67)$$

In a geothermal system, the pressure has little effect on minerals since it is relatively low. Therefore, the expressions can be simplified:

$$\Delta H^T = \Delta H_f^{P_r, T_r} + \int_{T_r}^T C_p dT, \quad S^T = S^{P_r, T_r} + \int_{T_r}^T \left(\frac{C_p}{T}\right) dT \quad (68)$$

The Gibbs free energy for a particular chemical reaction is

$$\Delta G_{\text{reac}}^T = \sum_i \gamma_i \Delta G_i^T \quad (69)$$

where

γ_i is the stoichiometric coefficient for each phase or gas species in the reaction;
 ΔG is the apparent modal Gibbs free energy of formation from the elements at temperature T of species i .

There is a relationship between the Gibbs free energy and equilibrium constant,

$$\Delta G_{\text{reac}}^T = -RT \ln K = -RT \sum_i \gamma_i \ln a_i \quad (70)$$

where

K is the equilibrium constant at temperature T ,
 a_i is activity of each species i in the reaction.

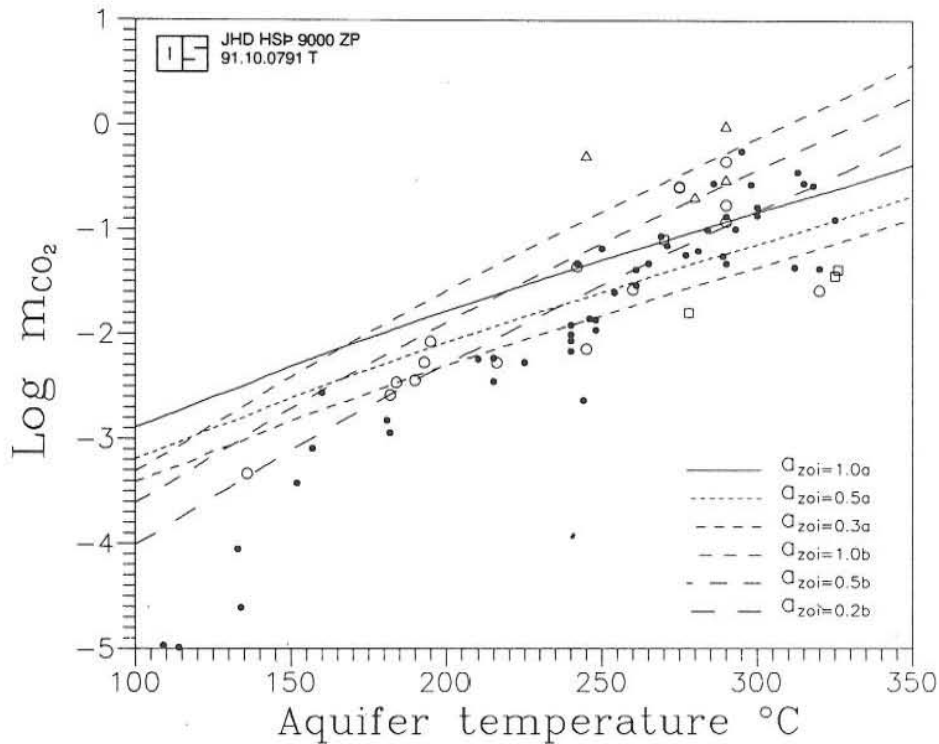
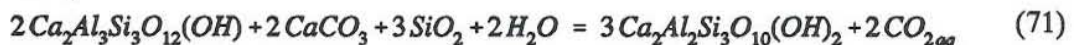


FIGURE 7: Mineral buffers for CO_2

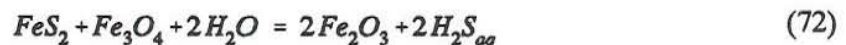
Figure 7 shows the chemical equilibrium between CO_2 and the zoisite + prehnite + calcite + quartz minerals buffer. The calculations do not lead to the same conclusion as Arnorsson and Gunnlaugsson (1985) reached in Figure 4 in their paper. The dots plotted represent data from Table 2 in the paper by Arnorsson and Gunnlaugsson (1985). The circles, triangles and squares plotted represent data from Table 3 in the same paper. Circles represent main inflow composition, squares extensive boiling in boreholes, and triangles are affected by magmatic activity. Curves a are based on thermodynamic data reported by Helgeson and Kirkham (1974) and Helgeson et al. (1978) with zoisite activity 1.0, 0.5, and 0.3, respectively. Curves b are, instead, based on zoisite and prehnite thermodynamic data reported by Berman (1988) with zoisite activity of 1.0, 0.5 and 0.2, respectively.



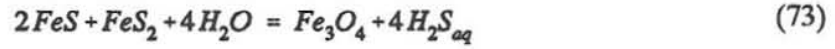
Most points plot near the curves. Many factors may cause deviation, e.g. analytical errors, inaccurate estimates of temperatures of main inflow, the effect of two phases, mixing, boiling and condensation during upflow, addition of magmatic gas, and so on. It is clear that the composition of some samples collected does not represent the composition of the original fluid due to extensive boiling and thus indicate low temperatures. The converse is true for a sample affected by magmatic activity.

Figure 8 shows the chemical equilibria between H_2S and several potential mineral buffers. All the thermodynamic data are from Helgeson and Kirkham (1974) and Helgeson et al. (1978). The symbols have the same meaning as in Figure 7.

Curve 1:



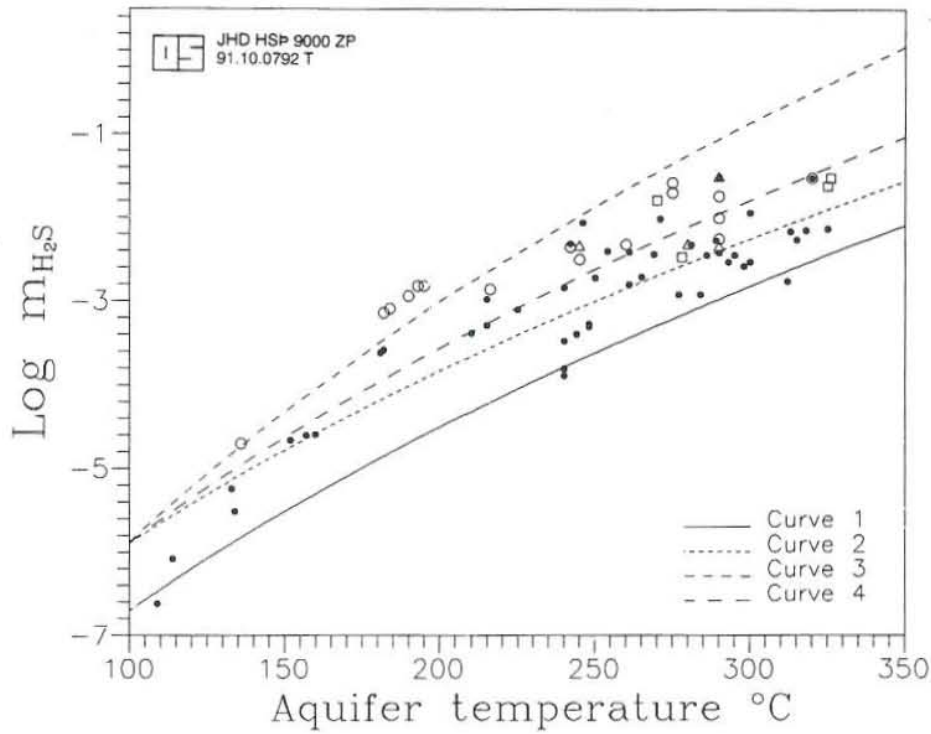
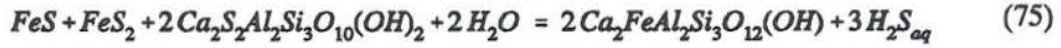
Curve 2:



Curve 3:



Curve 4:

FIGURE 8: Mineral buffers for H_2S

5. EVALUATION AND INTERPRETATION OF RESULTS FROM SELECTED GEOTHERMAL FIELDS

5.1 Krafla geothermal field

The active Krafla volcanic system and its associated fissure swarm is located in the northern part of the volcanic rift zone in Iceland. The Krafla high-temperature area is within the Krafla caldera, which was formed about 100,000 years ago. Volcanic activity is high in the area. The most recent eruptive period started in 1975. Nine eruptions were recorded in the following ten years with the last one taking place in September 1984 (Bjornsson, 1985). Geothermal manifestations are extensive in the Krafla area with fumaroles and mudpools spread over a large area. The high-temperature area can be divided into at least four fields; the Leirhnukur, Leirbotnar, Sudurhlidar and Hvittholar fields (Armannsson et al., 1989) (Figure 9). These fields, with the exception of the Leirhnukur field, have been exploited since 1975. The Krafla high-temperature system has proven to be a complex geothermal system (Armannsson et al., 1987). In Leirbotnar, the system consists of a relatively cool upper zone (190-220°C) and a hot lower zone (300-350°C). In the Hvittholar field the upper part is relatively hot (260°C at 600 m), and the lower part much cooler (180°C at 1200 m), gradually increasing to 240-250°C at 1800 m). The temperature in the Sudurhlidar field follows the boiling temperature-pressure curve at depth (Figures 10 and 11). Isotope and gas composition studies reveal that all geothermal fluids originate from relatively local meteoric precipitation and the fluids of both the Leirhnukur and Leirbotnar fields were affected by the magmatic activity in the form of an influx of magmatic gas into the geothermal system (Armannsson et al., 1989; Darling and Armannsson, 1989).

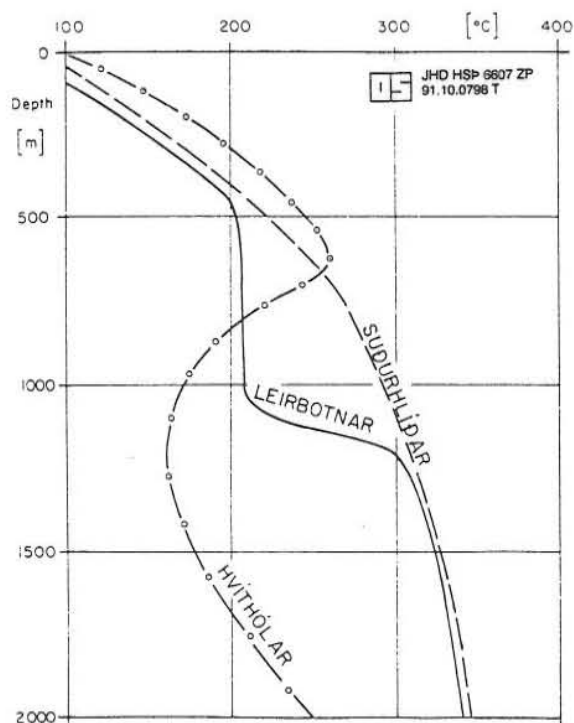


FIGURE 10: Simplified temperature profiles for the three exploited field in the Krafla area

The temperature in the Sudurhlidar field follows the boiling temperature-pressure curve at depth (Figures 10 and 11). Isotope and gas composition studies reveal that all geothermal fluids originate from relatively local meteoric precipitation and the fluids of both the Leirhnukur and Leirbotnar fields were affected by the magmatic activity in the form of an influx of magmatic gas into the geothermal system (Armannsson et al., 1989; Darling and Armannsson, 1989).

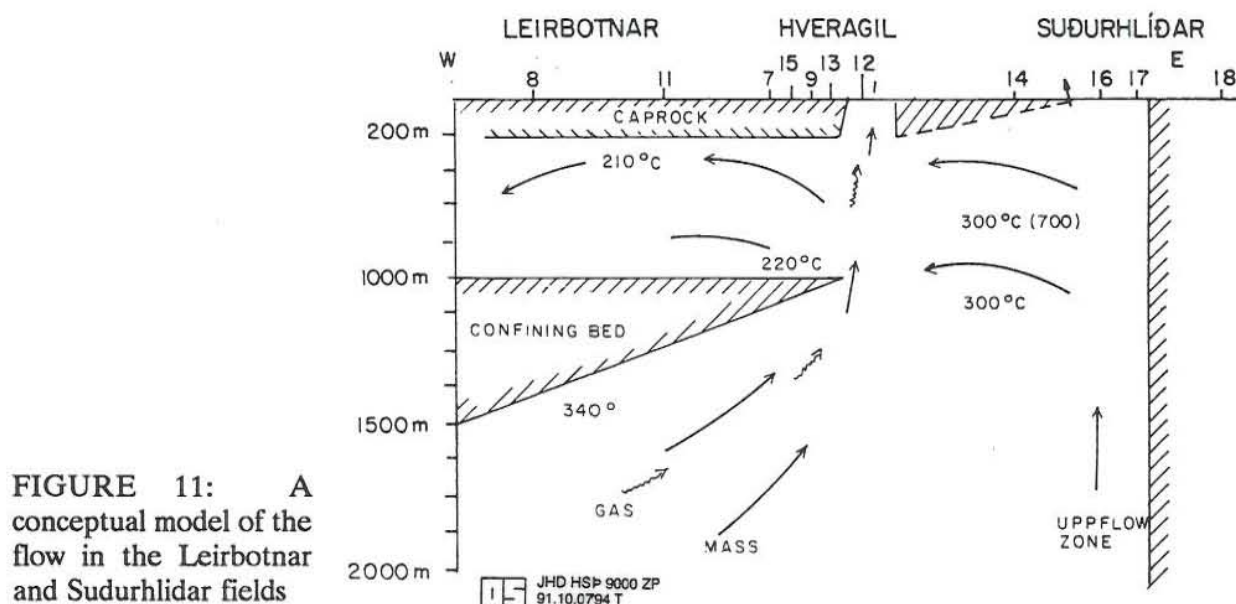


FIGURE 11: A conceptual model of the flow in the Leirbotnar and Sudurhlidar fields

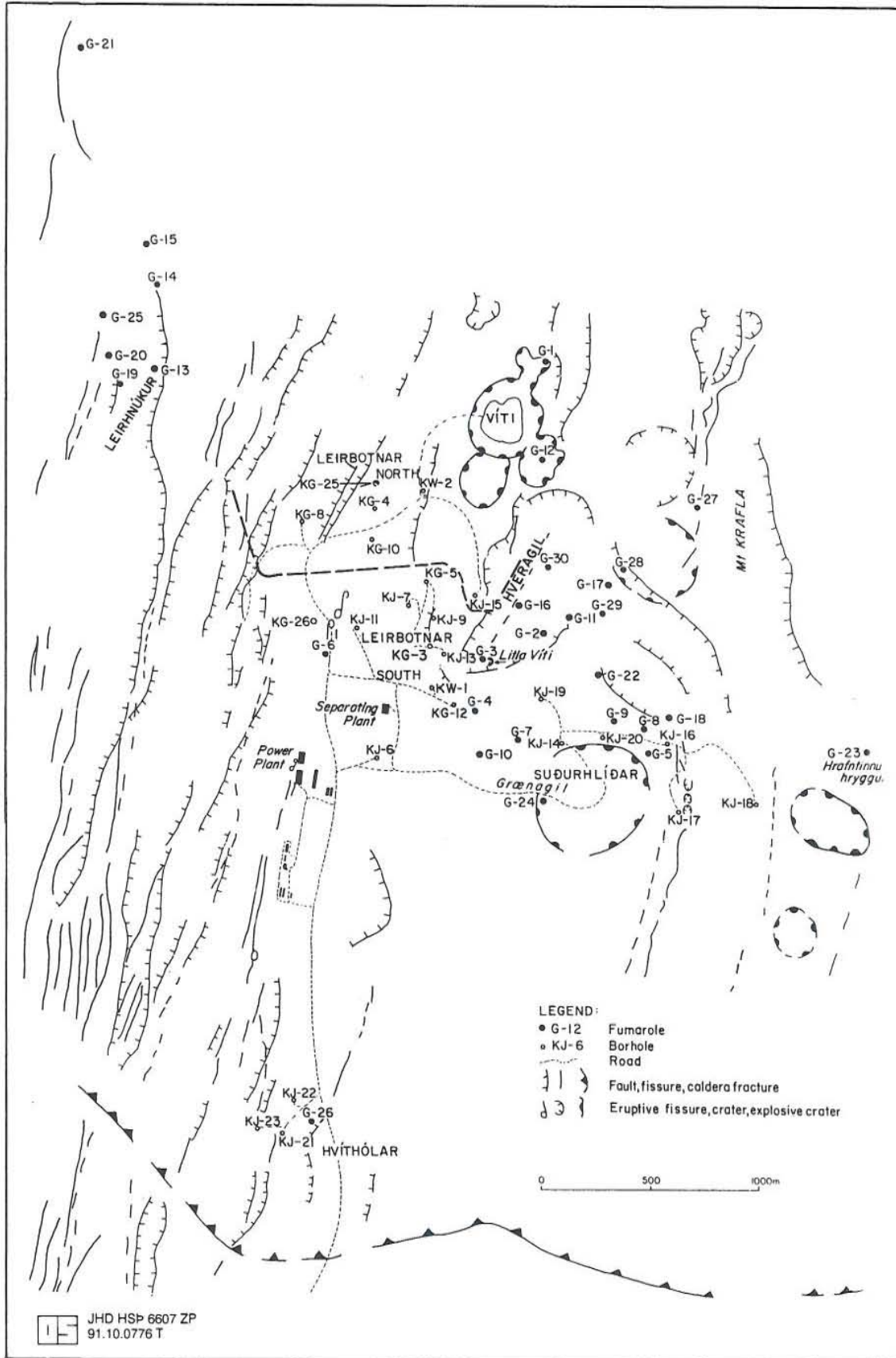


FIGURE 9: The locations of the wells and fumaroles in the Krafla area

TABLE 5: The chemical composition of geothermal fluid from selected fields

Location	Bakki BA-01	Hve H-8	Hve G-4	Hve G-6	Krafla K02	Krafla K03b	Krafla K11a	Krafla K14a	Krafla K26a	Krafla K26b
Sample No.	77- 0023	91- 9106	80- 0009	80- 0008	77- 1133	76- 0055	79- 1033	85- 1041	91- 1002	91- 1006
Sampling pressure(bar g)	0.8	6.2	5.7	5.5	4.2	1.7	12.5	11.6	2.3	2.7
pH/°C	8.79/20	8.98/21	9.04/23	9.31/23	9.29/21	8.08/27	7.53/23	8.51/23.9	9.70/21	9.56/24
SiO ₂	134	281	260	376	369	629	660	663	391	390
B	0.27	0.62	0.6	0.6	0.56	0.9	1.17	6.1	-	-
Na	398	152	167	177	207	196.8	187.4	163.4	203	206
K	21.6	12.4	12.5	18.2	14.4	31.8	25.4	32.7	24.2	25.7
Ca	76.3	2.51	2.26	2.3	1.98	1.7	1.5	0.47	3.0	2.55
Mg	0.03	0.064	0.001	0.001	0.01	0.01	0.001	0.032	0.054	0.047
Fe	0.02	0.005	0.01	0.01	0.02	0.01	0.05	0.07	0.02	0.006
Al	0.08	0.50	0.50	0.50	1.35	1.26	1.29	0.50	0.73	0.74
SO ₄	126.4	41.7	40.9	33.7	196	139.4	124.2	3.68	24.9	232.7
Cl	607	131.3	130.4	185.2	28.9	37	46.6	69.4	24.1	24.4
F	0.4	1.92	1.6	1.04	0.62	1.0	1.63	4.15	0.81	0.84
CO ₂	7.5	58.8	54.1	32.9	89	253.8	246	160.4	55.5	58.3
H ₂ S	0.14	18.2	20.9	20.1	38	9.5	20.3	64.4	22.2	28.9

For the corresponding steam composition see Table 1 and enthalpy see Table 3;
Hve: Hveragerdi; -: not measured.

The hot water chemical composition for selected Icelandic wells is listed in Table 5. The main inflow in wells K02 and K26 comes from the upper zone in the Leirbotnar field, which was not affected by magmatic activity. The 1977 sample from K02 was, thus, not affected by magmatic gas (Tables 1 and 2). The calculated CO_2 -, H_2S -, H_2 - and CO_2/H_2 - temperatures for the sample from K02 are slightly higher than that of the estimated inflow (193°C). Figure 12 is a mineral equilibrium diagram for data on well K02 calculated using the WATCH program (Arnorsson et al., 1982). All probable primary, secondary and alternative minerals are considered. The geothermometer temperatures with respect to quartz are 211°C, to chalcedony 191°C and to Na/K 160°C (Table 6). Most of the minerals attain equilibrium between 180 and 210°C. In this range, the system is over-saturated with respect to pyrite (not drawn). The mineral buffers, which probably control the gas concentrations should, at least, show a rapid change in log (Q/K) for one mineral near the equilibrium temperature range, and its behaviour should be as predictable as that of an indicator used in chemical analysis. The potential mineral buffer for H_2S is pyrite + magnetite + epidote + prehnite. Using this mineral buffer, and inserting into the thermodynamic equation the H_2S concentration in total discharge, results in a temperature of 207°C. This is in good agreement with the mineral equilibrium temperature of Figure 12. It is difficult to calculate the CO_2 temperature on the basis of quartz + calcite + zoisite + prehnite mineral buffers due to uncertain values for mineral activity. Well K26 is new and started to discharge on September 2, 1991. Two samples were collected, after one and four days discharge, respectively. Temperature logging revealed that the main inflow temperature had changed a little between the two sampling times, i.e. from 190 to 195°C. The increase in enthalpy can be seen in Table 3 and if it is stated that water flow did not change much during this time, the inference is increased steam flow. There is no difference in the water composition of the two samples except in the iron concentration. The high iron concentration of the first sample is suspected to be caused by contamination by equipment. The mineral equilibrium diagrams for samples K26-a and K26-b are shown in Figure 13. Figure 13a reflects the thermal fluid contaminated by circulation water, which entered the aquifers during drilling and well testing. Figure 13b shows that most mineral equilibria focus in the range 195 to 208°C. Quartz, chalcedony and Na/K temperatures are 212, 193 and

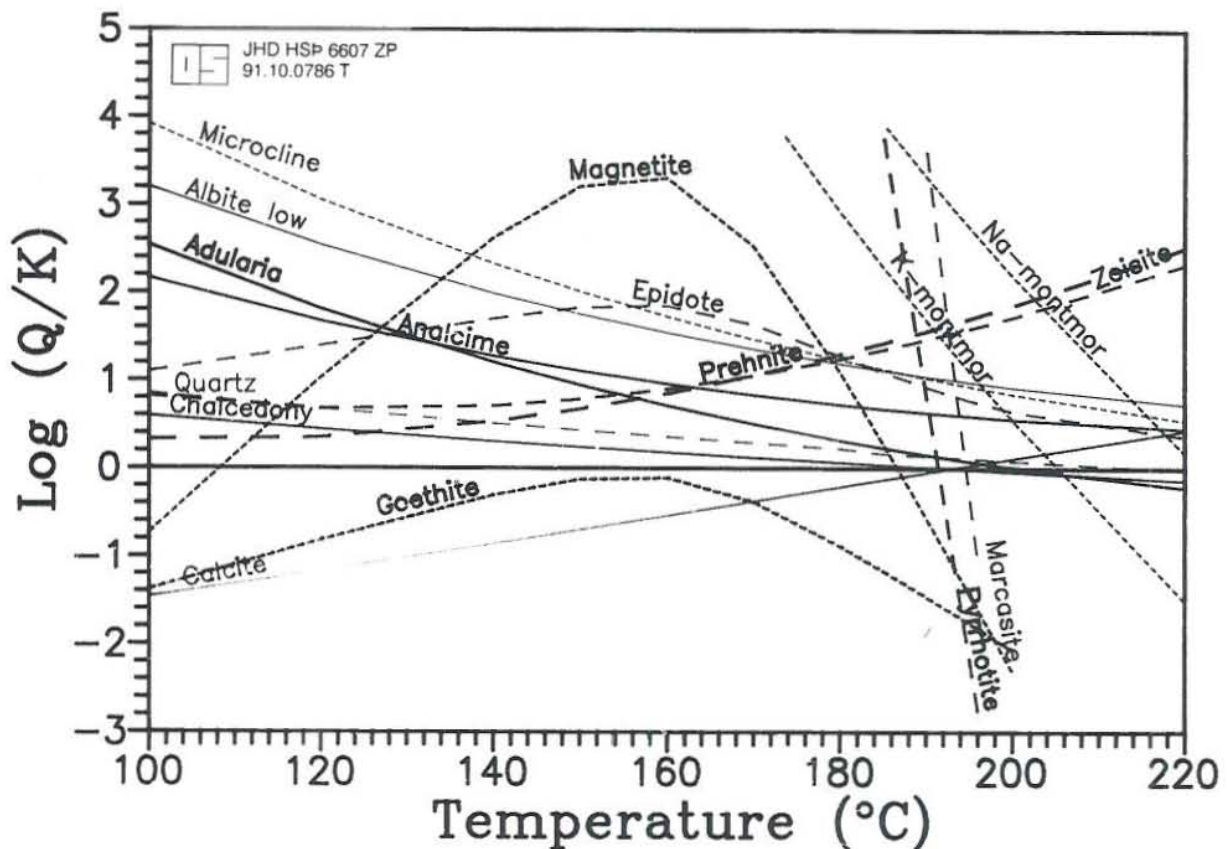


FIGURE 12: Mineral equilibrium diagram for Krafla well K02

214°C, respectively. The temperature calculated from the H_2S mineral buffer is 207°C. The behaviour of calcite in solution changed from supersaturation to undersaturation due to an increased boiling portion in the well between the two collection times. The results for sample K26b are more reasonable, given the reliable temperatures obtained by the H_2S , H_2 and CO_2/H_2 geothermometers (Table 2). Any discrepancies may be due to different solubilities and reaction kinetics during boiling.

TABLE 6: Comparison of temperatures obtained by solute geothermometers and those obtained using a mineral buffer (°C)

Well no.	Quartz	Chalcedony	Na/K	Mineral buffer for H_2S
Bakki BA-01	144	122	141	136
Hvalfjörður H-1	158	129	136	148
Hveragerði H-8	194	173	179	193
Hveragerði G-4	188	167	171	195
Hveragerði G-6	203	183	204	205
Krafla K02	211	192	160	207
Krafla K26	212	193	214	207

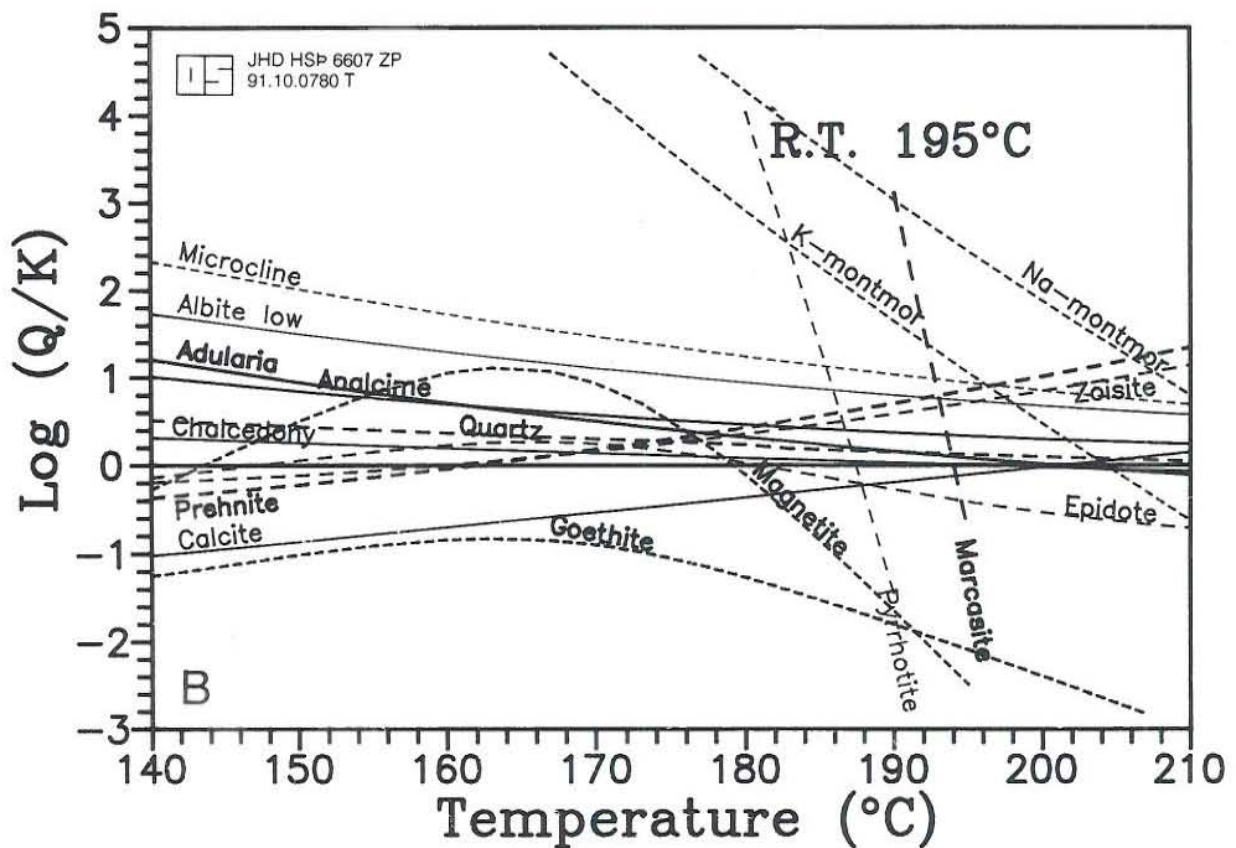
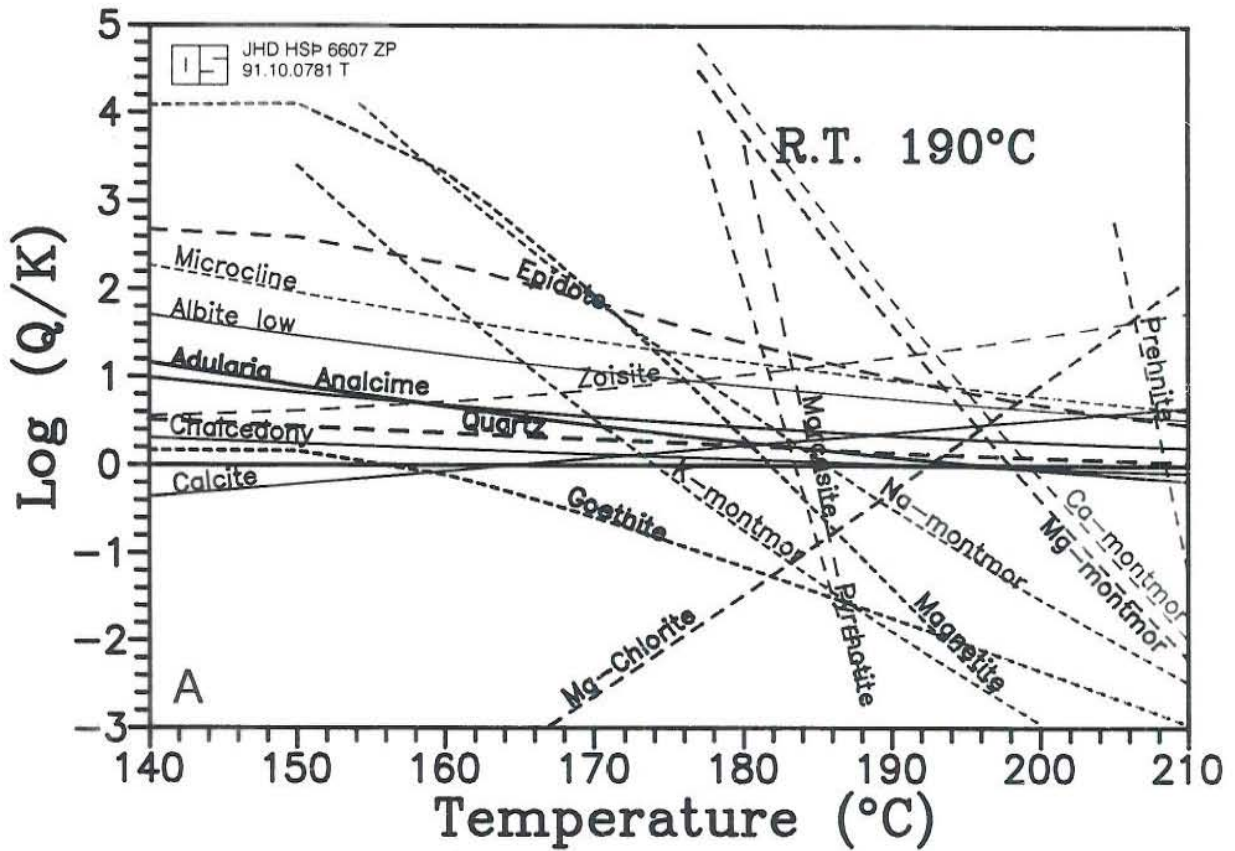


FIGURE 13: Mineral equilibrium diagrams for Krafla well K26; samples collected after A) one day's discharge, B) four days discharge

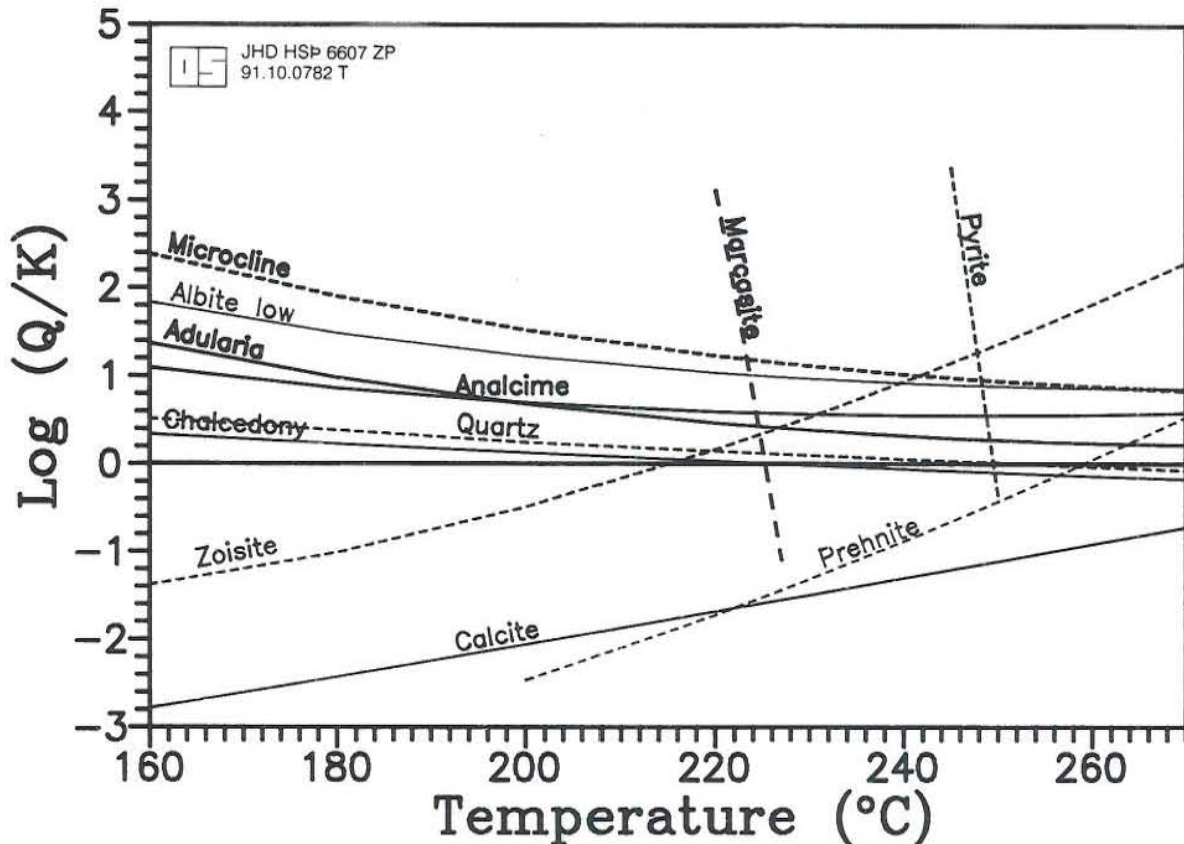


FIGURE 14: Mineral equilibrium diagram for Krafla well K03

Two samples from well K03 were considered. Sample K03-a was collected prior to any observed magmatic activity in the area, and can be considered to represent undisturbed conditions. The K03-b sample was collected in 1976, after the influx of magmatic fluid into the reservoir. The main effect is an increase of carbon dioxide and hydrogen sulphide in steam. The results for K03-a give reasonable H_2S - and H_2 - temperatures, a slightly low CO_2 - temperature and a relatively high CO_2/H_2S - temperature. The disturbed sample shows a very high CO_2/H_2S ratio, high CO_2 - and low H_2S - and H_2 - temperatures, all of which reflect the dominance of the magmatic CO_2 in the reservoir gas. The H_2S - temperature has not changed a lot. Figure 14 shows that the mineral equilibria are disturbed by the magmatic fluid. There are no log (Q/K) values concentrating in a narrow temperature range. Excess CO_2 entering the reservoir causes calcite to become under-saturated and the formation of an unstable geochemical system. New equilibria will be approached gradually after the end of magmatic activity.

The 1977 sample from well K10 was collected from the area of maximum magmatic activity during the peak period. Compared to K03-b, the gas concentration in the steam has increased. The geothermometer temperature is high for CO_2 , low for H_2 and CO_2/H_2 , but the H_2S - temperature is in good agreement with the estimated mean temperature of inflow, 290°C. The results for the samples from K07 and K11 reflected the behavior of a geothermal system affected by magmatic fluid followed by recovery to a new thermodynamic system.

There is a difference between the compositions of K07-a and K07-b. The CO_2 - temperature declined quickly, that for H_2S one was relative stable and the H_2 - temperature increased. During the same period, the mean inflow temperature declined from 280 to 260°C. The CO_2 - temperature decreased a lot, but that for H_2S and H_2 were relatively stable and low. The CO_2/H_2S

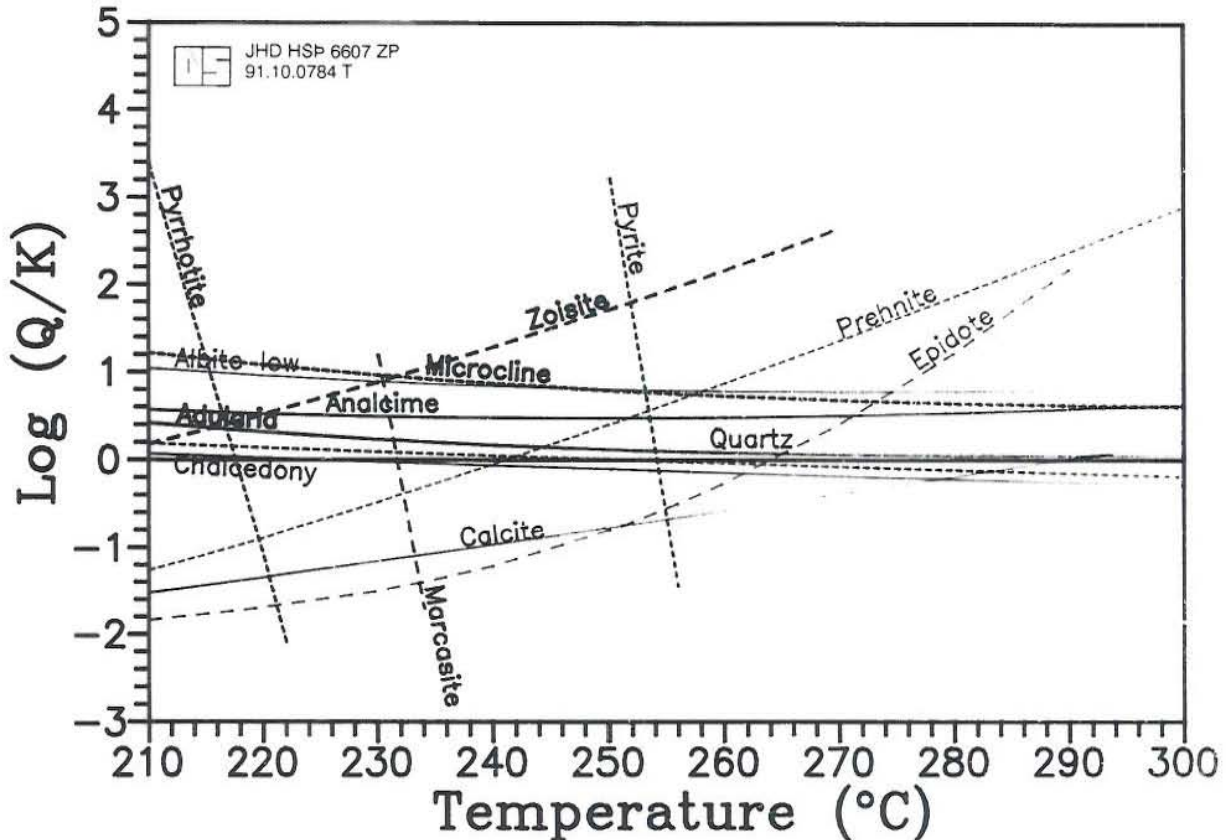


FIGURE 15: Mineral equilibrium diagram for Krafla well K11

ratio decreased. The behavior of the liquid in well K11 was similar. The mineral equilibria for K11-a are shown in Figure 15. No minerals reach equilibrium over a narrow range. It is difficult to discuss a change in the H_2S/H_2 ratio, because both gases are relatively unstable and probably removed from the steam at different rates during their rise to the surface. The location of fumarole G6 is near to well K11. The CO_2 content of the steam is similar, but the H_2S and H_2 content is lower in steam from G-6 than from K11-b, which was collected at the same time. The high nitrogen content reflects an atmospheric origin. Low H_2S and H_2 contents are considered to be due to removal from steam during steam ascent to the surface. There are two main aquifers in well K25, a hot lower zone aquifer with a fluid composed mainly of steam and a cooler upper zone with one phase (liquid) inflow. The average inflow temperature is $270^\circ C$, 55% from the lower zone and 45% from the upper zone (Armannsson and Gislason, 1991). The CO_2 and H_2S geothermometers were considered to represent a mixing temperature. The low value obtained from the H_2 geothermometer is thought to be derived from the upper zone fluid.

Wells K14 and K20 are in the Sudurhlidar field, which was not affected by magmatic activity. The composition of the fluid from well K14 is quite stable. Several aquifers are found in the well, with an average temperature of $275^\circ C$. Gas geothermometers give a high CO_2 - temperature, slightly low H_2S - and H_2 - temperatures and a lower CO_2/H_2 - temperature. The geothermal fluid has boiled extensively in the borehole. The mineral equilibrium for extensive boiling is shown in Figure 16. It reveals that mineral equilibrium temperatures are scattered over a wide range; the lowest one is obtained for magnetite, the highest for Na-montmorillonite. The calcite temperature reflects the actual temperature of inflow. It probably reflects that the fluid collected at the wellhead cannot represent the composition of the fluid in the reservoir. The same applies to well K20 except that there a high gas/steam ratio is observed. Fumarole G5 is near well K20 and its

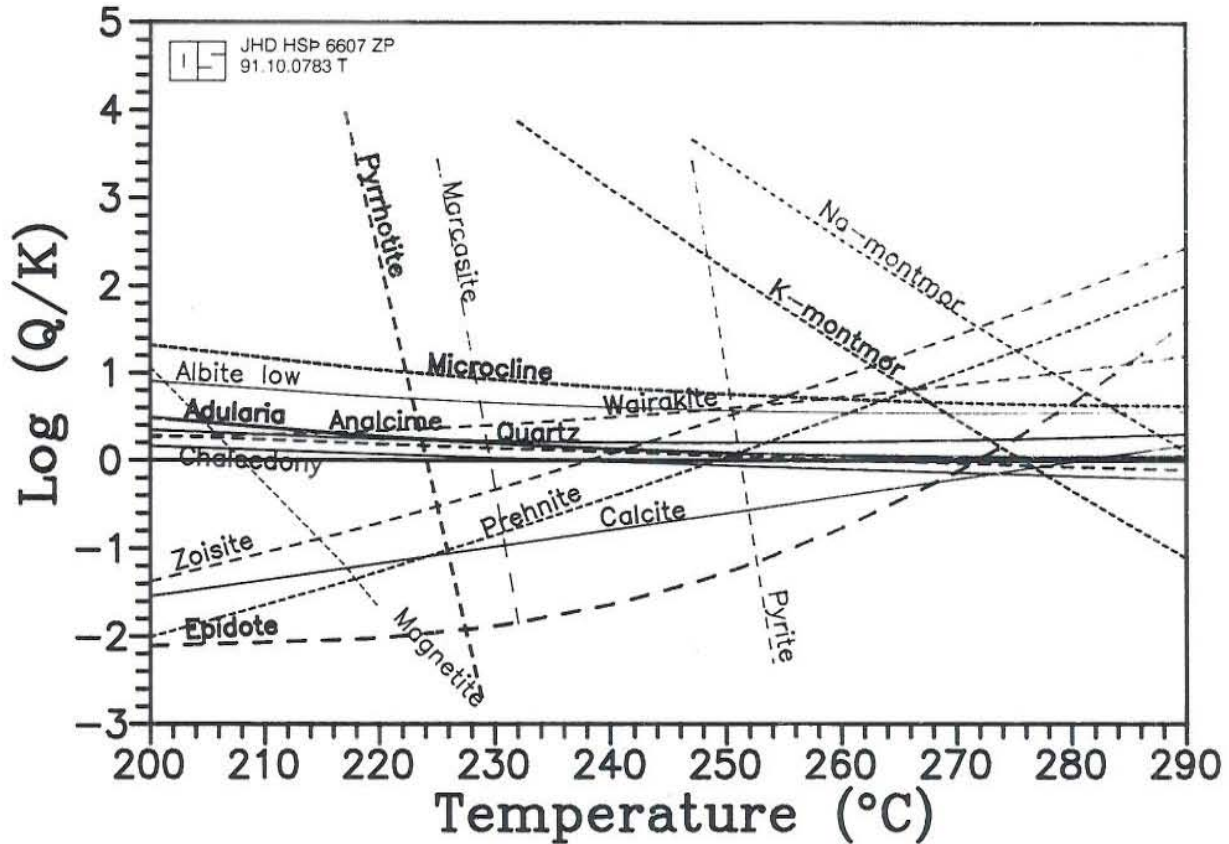


FIGURE 16: Mineral equilibrium diagram for Krafla well K14

composition has been monitored for a long time. The gas/steam ratio has been found to increase, which leaves gas geothermometer results based on gas ratios unchanged. This tendency probably reflects more extensive boiling in the reservoir during exploitation.

The calculated temperatures for fumarole G26 in the Hvítholar field are 289°C for the CO_2 -, 232°C for the H_2S -, 253°C for the H_2 -, and 224°C for the CO_2/H_2 - geothermometers. Compared to the main inflow into well K22, which is in the range of 180 to 260°C, this is considered to be in reasonable accord with measured temperatures except that the CO_2 - temperature is slightly high, probably because of condensation of steam.

Fumarole G19 is located in the Leirhnukur field. No well has been drilled there so far. The variation in its steam composition has been monitored since 1979. It is clear that the gas content, aside from that of N_2 , is decreasing with time. It seems to indicate that the deep reservoir was disturbed by magmatic emanations and has recovered gradually. The calculated temperature for the 1990 sample is consistent with pre-magmatic temperatures, and likely to indicate the subsurface temperature.

5.2 Other high-temperature fields in NE-Iceland

Fremri Namar: The Fremri Namar field is within in the Ketildyngja volcanic system on the next fissure swarm to the east of the Krafla swarm. The geological formations in this area are mainly hyaloclastites, but the east part is rhyolite. The area was formerly used as a sulphur mine. The CO_2 temperatures reflect its maximum probable temperature, 310°C and only the H_2S and H_2 may

approach the actual temperature (Table 2).

Namafjall: The geological conditions of the Namafjall field are similar to those of the Krafla field as the field is within the Krafla fissure swarm. Studies on the discharge from well B11 show that H_2S -, H_2 -, CO_2/H_2 - and H_2S/H_2 - temperatures represent the situation in the deep reservoir. The CO_2 concentration indicates a relatively low temperature. The gas concentration of selected fumarole steam is slightly higher than that of well B11 steam. It could be inferred that condensation occurred in the fumaroles.

Theistareykir: The Theistareykir field is within the Theistareykir volcanic system on the next fissure swarm to the west of the Krafla swarm. Surface geothermal manifestations are abundant. The geological situation and studies on gas chemistry are discussed in detail by Armannsson et al. (1986). The isotopic composition of steam from fumaroles is described and a condensation model for isotopic composition invoked to explain the results for a part of the field by Darling and Armannsson (1989). Steam collected in 1981 and in 1991 from fumaroles G1, G3 and G6 shows that some changes have taken place. The results for gas composition indicate that the subsurface temperature is in the range of 191-290°C. Taking into account the condensation coefficient suggested by Darling and Armannsson (1989), the corrected CO_2 - temperatures for samples G-6a and G-6b are 231 and 210°C, respectively. The Theistareykir field has not been exploited yet.

5.3 Low- and high-temperature fields in SW-Iceland

Bakki: The Bakki low-temperature field is located in the Olfus Region in South-Iceland. It is on the eastern flank of the southwestern active volcanic rift zone. Two wells have been drilled in the Bakki geothermal field. The water is saline, possibly influenced by seawater (see Table 5). Well BA-01 was drilled in 1977 and is 886 m deep. The hyaloclastites and basalts observed in the well are altered from 75 m depth to the bottom. Calcite, zeolite, pyrite, green-blue clay, chlorite and epidote are found in the borehole cuttings from the well. The main inflow temperature, according to logging, is about 136°C (Figure 17a). The temperature estimated from the H_2S component is in good agreement with the measured one. Other temperatures obtained by gas geothermometers deviate at least 30°C from the measured one (Tables 2 and 4). The selected solute geothermometers yield temperatures in the range of 122 to 144°C (Table 6). The temperature calculated from H_2S mineral buffers is within the range of mineral equilibria (Figure 18).

Haedarendi: A high CO_2/H_2S ratio in steam is found in well H2, located in the Haedarendi low-temperature field, in the Southern Lowlands of Iceland. The powerful aquifer was encountered at the bottom of the hole in an altered basaltic layer. The maximum measured temperature is 154°C, and compares well with the chalcedony temperature. Most gas geothermometers are invalid for this situation where the CO_2/H_2S ratio is more than 100. Results approaching the measured temperature are obtained from H_2S - and *FT* reaction geothermometers.

Hvalfjordur: The inferred inflow temperature (well H-1) is about 150°C, based on logging. The studies on lithology reveal that alteration is very intense and alteration minerals include calcite, laumontite, pyrite, and epidote. Basalt predominates in the deeper parts, but hyaloclastite is more pronounced in the shallow parts. The temperatures obtained from solute geothermometers and mineral buffers are shown in Table 6; the latter agrees well with the inferred temperature.

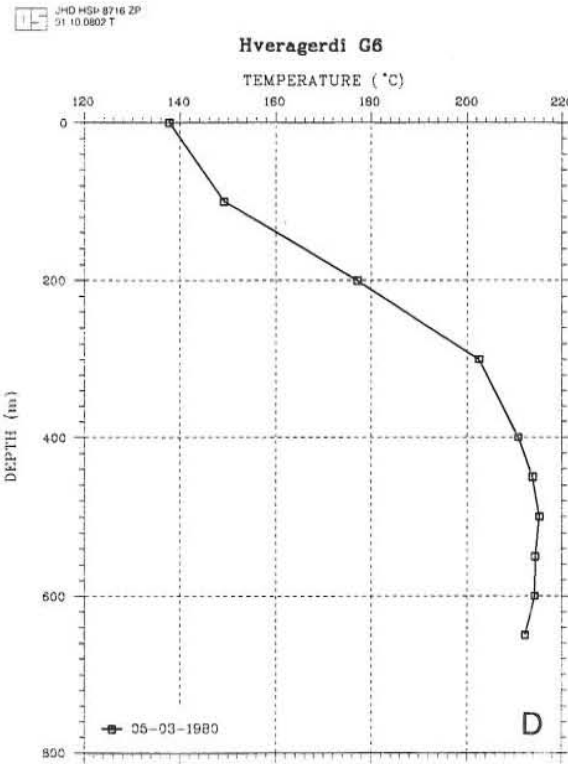
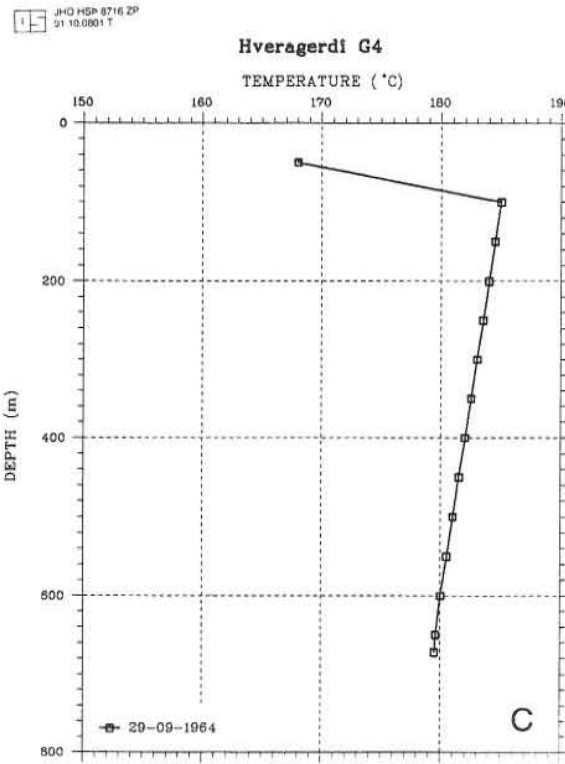
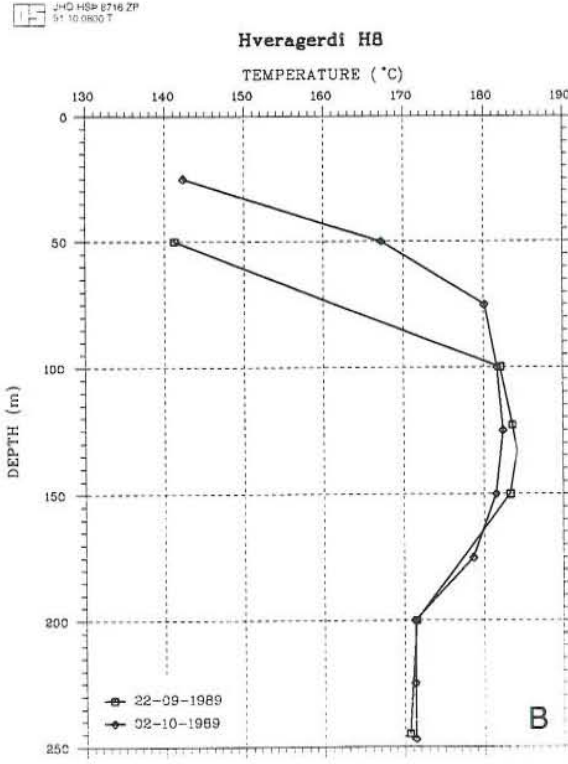
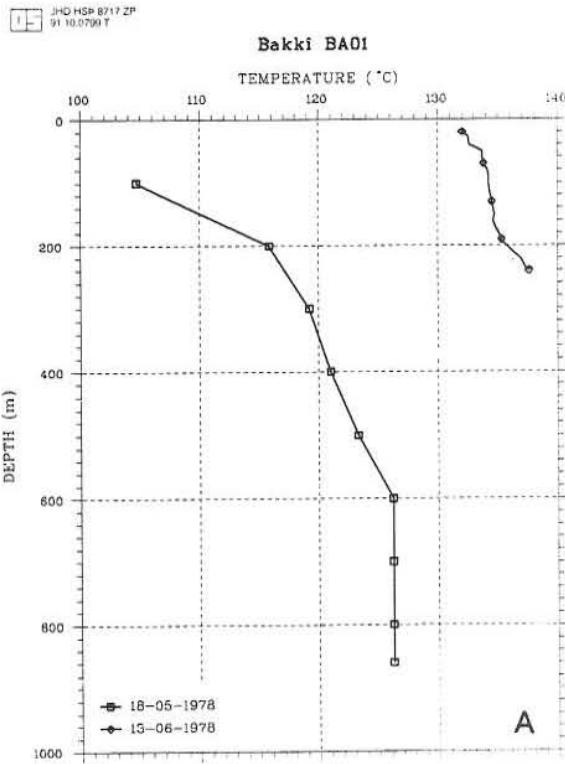


FIGURE 17: Results of temperature measurements for A) Bakki well BA-01; and Hveragerdi B) well H-8, C) well G-4 and D) well G-6

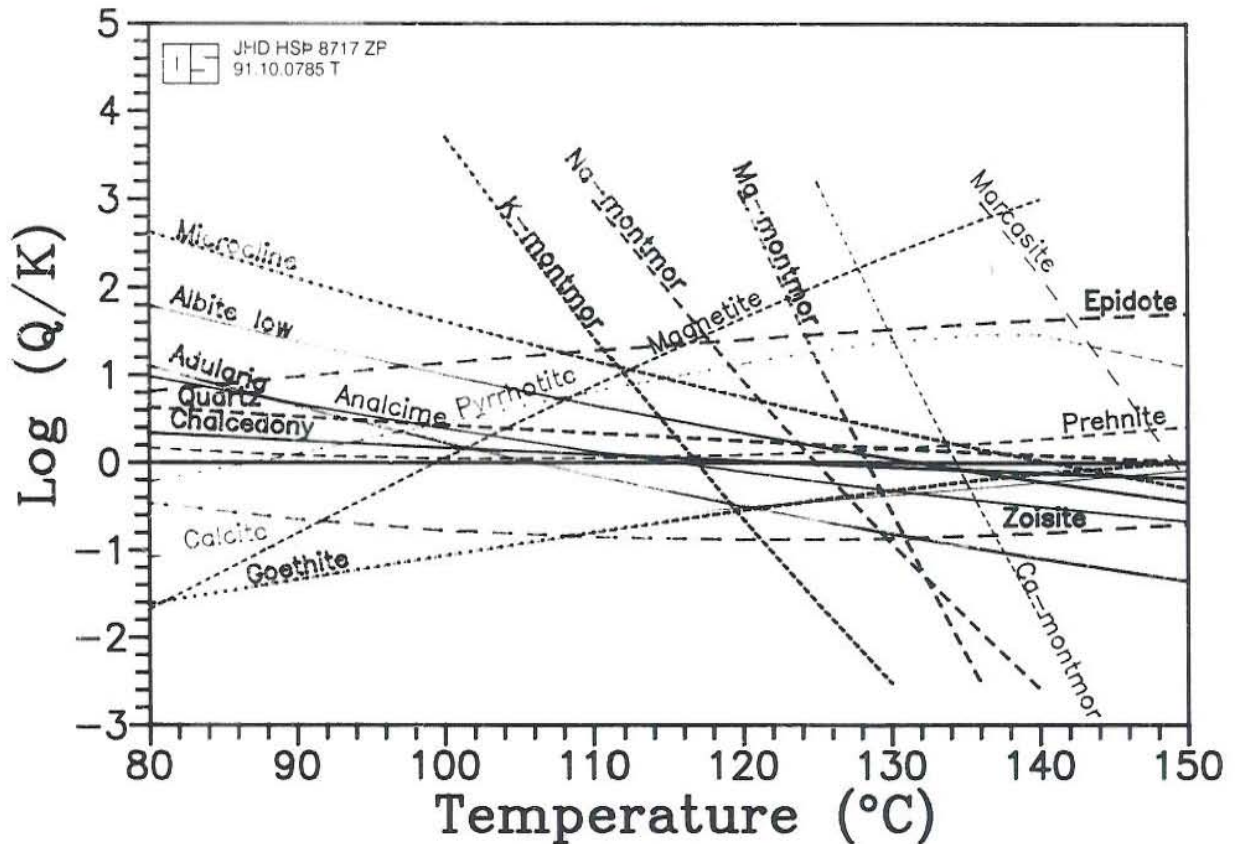


FIGURE 18: Mineral equilibrium diagram for Bakki well BA-01

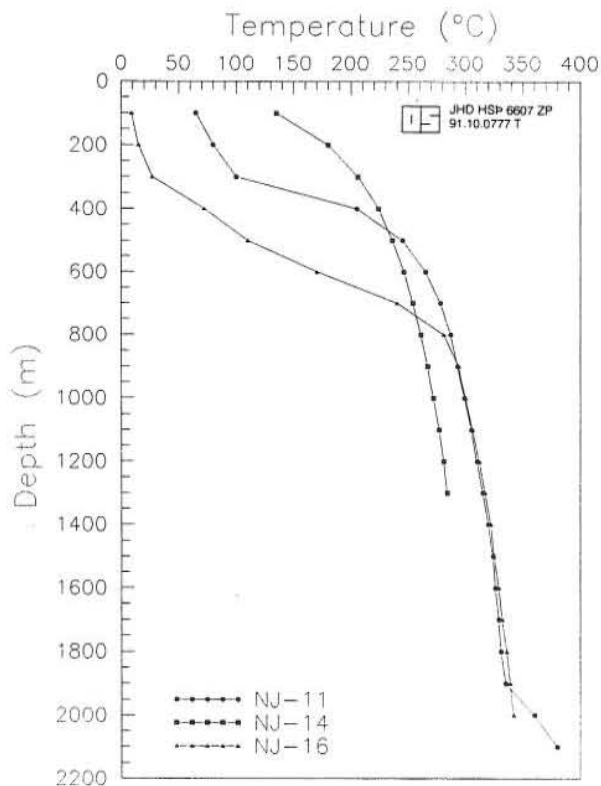


FIGURE 19: Temperature measurements for Nesjavellir wells NJ11, NJ14 and NJ16

Nesjavellir: The Hengill high-temperature geothermal area is located within the southwestern volcanic rift zone in Iceland. It is one of the largest geothermal areas of Iceland and is characterized by tensional stress parallel to spreading direction. The Nesjavellir field is found in the northern sector of the Hengill central volcano. In the uppermost 500 m, hyaloclastites dominate the rock sequence; below that, basaltic lava flows occur. Magmatic intrusions become more frequent with depth. At 1400-1600 m depth, they become the major rock components. Temperature curves for wells NJ11, NJ14 and NJ16 are shown in Figure 19. Several aquifers feed these wells whose relative flows are not known exactly. The measured enthalpy of the fluids is higher than that expected from one-phase liquid flows in the aquifers at the measured temperatures. The mechanism is probably the heating of a relatively cool fluid by convection followed by boiling; during its rise to the wellhead. Most of the steam is thought to come from the deep part; the average H_2S , H_2 , CO_2/H_2 and H_2S/H_2 temperatures are in good agreement with the measured temperature in the

deep part. The fumaroles N44, N46, N48 are to the southeast of well NJ14. The gas concentration in their steam is higher than in well NJ14 and presumably indicates a deeper reservoir temperature than that observed in the well.

Hveragerdi: The Hveragerdi geothermal field is located on the southeastern margin of the Hengill area and the volcanic rift zone. All strata are late Quaternary volcanics. The inflow into wells G-6, G-4 and H-8 (Figure 17) is considered to be from the same general regional flow, only it comes later into wells G-4 and H-8 at a stage where it has become cooler. The behaviour of possible minerals in these wells is demonstrated in Figures 20, 21 and 22. It is obvious that there is a marked change in the log (Q/K) value near the measured temperature according to the diagrams. The fluid remained over-saturated with respect to pyrite. Fumaroles G29 and G30 are closest to G-6 and might be expected to suggest a hotter fluid than P68 which is nearer to the village and the cooler wells. One possible reason for the relatively high temperature obtained for these fumaroles is condensation. As this does not affect ratios, it is interesting to note that the CO_2/H_2 - temperature (t_7) is lower for P-68 than the other two, supporting the above contention.

5.4 Kenyan geothermal fields

Calculated gas temperatures for well no. 6, Olkaria, Kenya, really represent subsurface temperature (Tables 2 and 4). Fumarole F22 could be regarded as belonging to the Olkaria geothermal system. The CO_2 temperature is high, and the H_2S temperature is low, probably due to removal of H_2S as steam ascends to the surface. The CO_2 temperature probably shows that the reservoir is affected by mantle-derived gas. The other two belong to different geothermal systems in the Rift Valley, F23 Longonot and F13 Suswa, but results appear to be similar. In this situation, the H_2 temperature is expected to be approximately close to main inflow temperature. No wells have been drilled in these two areas.

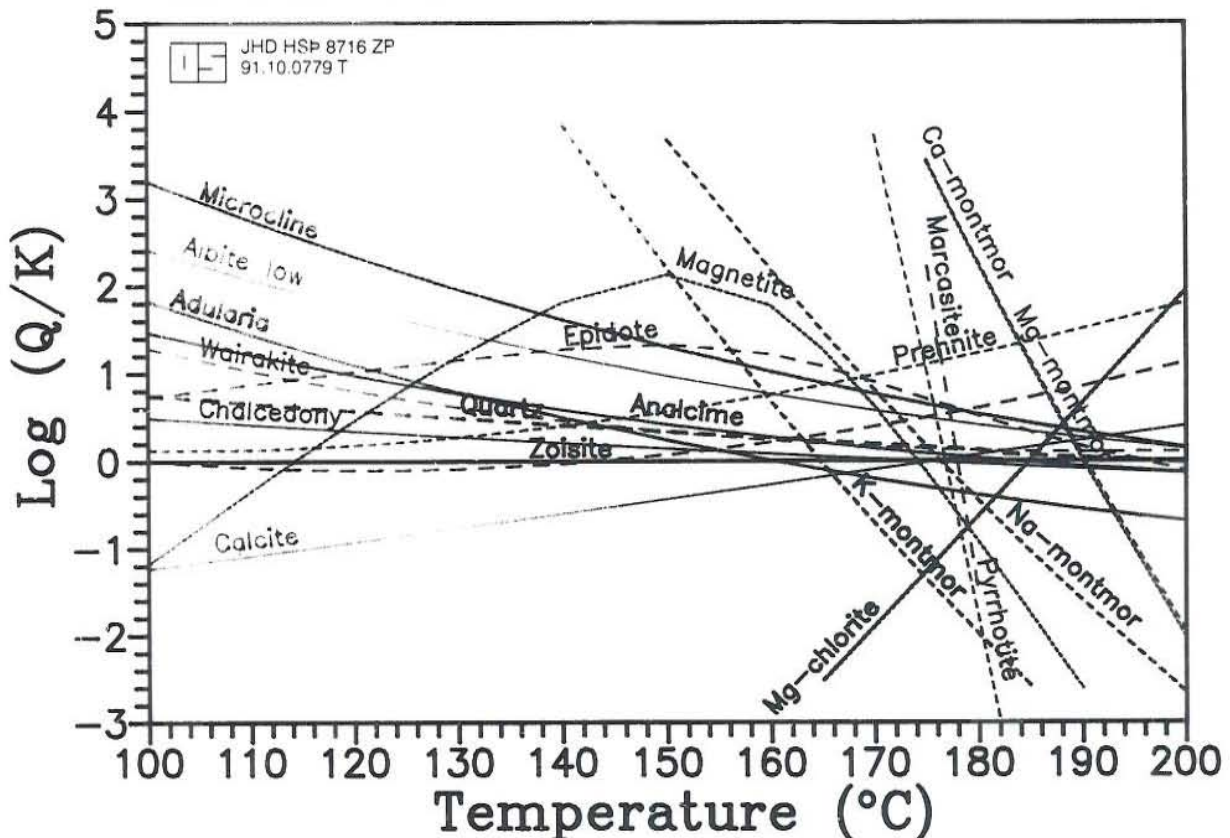


FIGURE 20: Mineral equilibrium diagram for Hveragerdi well H-8

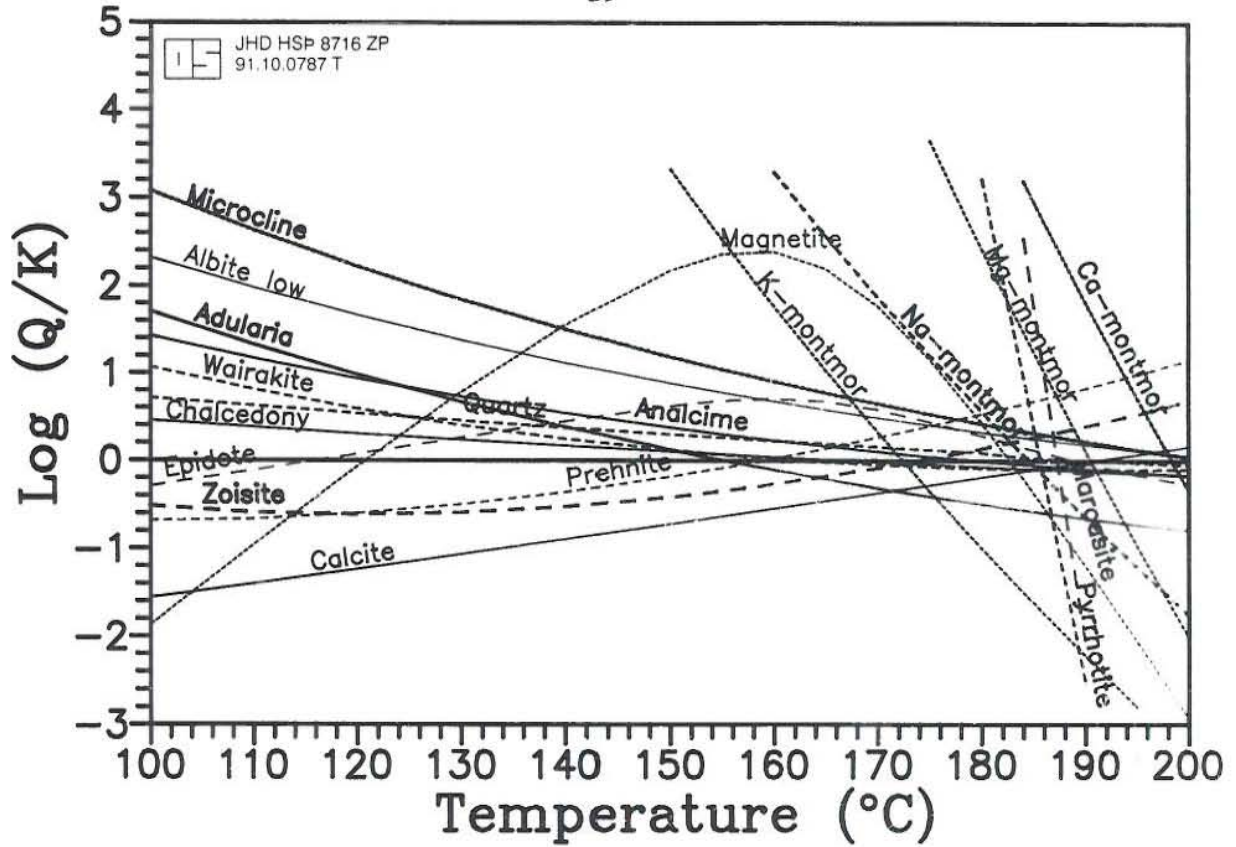


FIGURE 21: Mineral equilibrium diagram for Hveragerdi well G-4

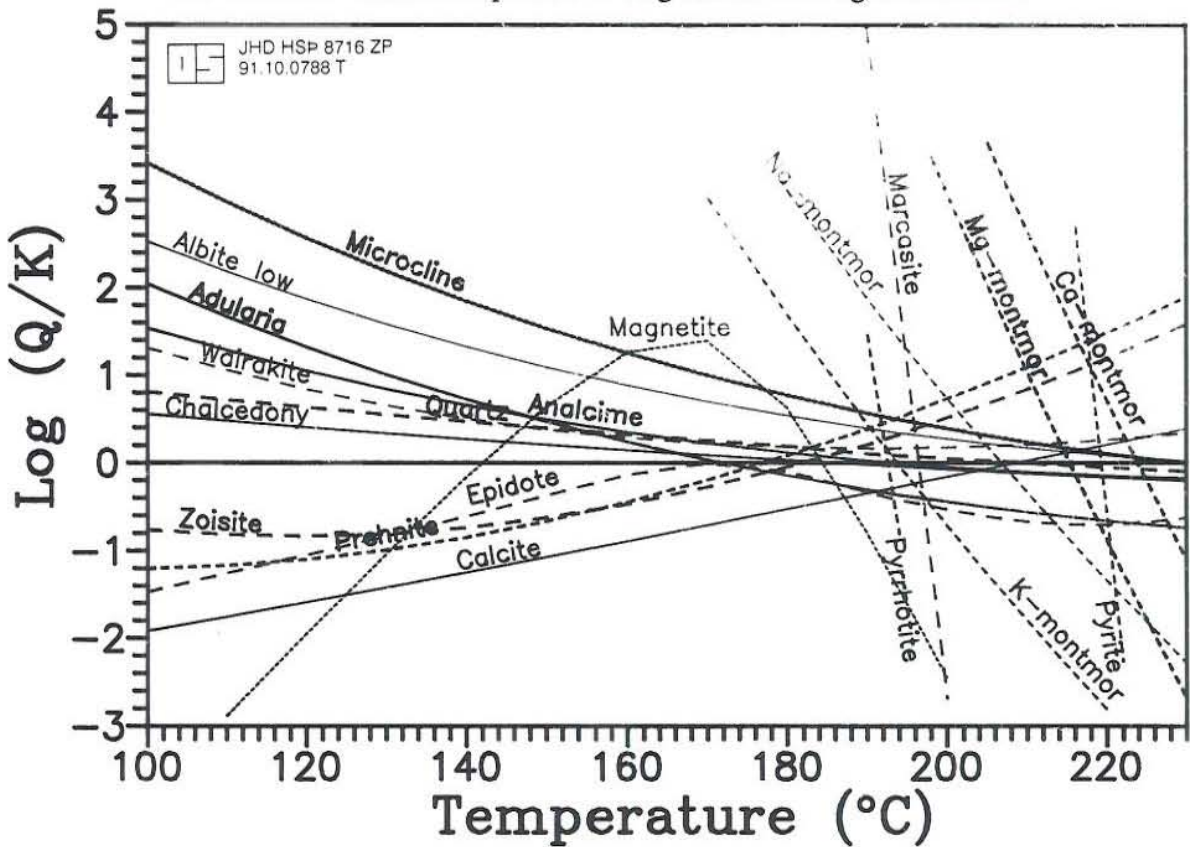


FIGURE 22: Mineral equilibrium diagram for Hveragerdi well G-6

5.5 The usefulness and limitations of individual gas geothermometers

It is difficult to select the carbon dioxide partial pressure parameter, when the geothermometer of Tonani (1973, 1980) is applied. It is not reasonable to consider only three possibilities, since widely differing temperatures are obtained for the three. Samples K03b, K07a, K10 and K11 were considered to have been affected by magmatic gas. Only sample K11a yielded a temperature close to the one measured when PCO_2 was selected to be 10 atm. Also, it is improbable that carbon dioxide pressure will reach 10 atm in reservoirs. D'Amore and Panichi (1980) proposed a gas geothermometer based on an empirical oxygen fugacity function and selected empirical CO_2 partial pressures. Calculated values were compared to ones measured in wells and this geothermometer often gave very high values. Arnorsson (1990) pointed out that one possibility is that these high temperatures truly reflect those existing at depth in geothermal reservoirs and another possibility he favoured is that this geothermometer does not apply accurately to all geothermal systems due to incorrect assumptions. Nehring and D'Amore (1984) suggested several non-empirical methods to evaluate subsurface temperature in one-phase liquid reservoirs. The inflows in wells BA-01, H08, G04, G06 and K26 considered for Table 4 are one-phase, but the results obtained by these methods are not satisfactory. The reason is that they assume the existence of several reactants including species (such as graphite) for whose existence at depth in these fields, there is no evidence. Thus they are invalid for Icelandic geothermal systems. Both temperature and initial steam fraction can be calculated using the method of D'Amore and Truesdell (1985) (Table 4 and Figure 5). It is suited for a one phase liquid geothermal systems. The results are reasonable for high-temperature fields. Wells K11, K10 and K07 were subjected to the inflow of magmatic gas (see section 5.1). The main inflow in well K11 is from the lower zone with temperatures from 280-310°C. The *FT-HSC* diagram yields results in agreement with the actual inflow temperature, even with magmatic gases added for this well, as well as for wells K07 and Olkaria-6, Kenya. There was no excess CO_2 in the reservoir, when sample K03a was collected. A good *FT-HSC* result is obtained for K03a and not for K03b, which contained excess CO_2 . Well K10 includes a relatively cool upper component and was also subjected to a magmatic gas influx, but the result reflects the temperature of the lower zone. The steam from K25, as mentioned above, is mainly from the lower zone and gas temperatures reflect this original source. It seems reasonable to consider that the Fischer-Tropsch reaction approaches equilibrium in the lower zone, the Leirbotnar field, Krafla. As mentioned above, the temperature in the Sudurhlidar field follows the boiling temperature-pressure curve at depth. The steam fraction at wellheads is high in this field. The steam composition from well K14 seems stable and high enthalpy and high hydrogen concentration were found for the steam from both K14 and K20. Relatively low temperatures and high steam fractions probably suggest inflows from depth mixing with upper inflows, causing the latter to boil. The steam fractions calculated from enthalpy and that temperature are 0.9, 0.91 and 0.60 for samples K-14a, K-14b and K-20, respectively. Another possibility is that the composition of the discharge does not represent the one in the reservoir since extensive boiling may cause a different upflow-rate for steam and for hot water. This could account for the results obtained from wells B11, N11, N14 and N16. In such a situation, thermodynamic methods cannot be used, because their basic assumptions are not met.

The Fischer-Tropsch reaction cannot be used as an independent geothermometer. In low-temperature fields, the chemical reaction does not approach equilibrium in reservoirs, and at high temperatures, the possibility of two phases must be considered.

Evaluation and interpretation of the nitrogen-carbon dioxide method (Arnorsson, 1987) is difficult. The nitrogen is a major component in the atmosphere and samples are easily contaminated by air. Also, when thermal fluid mixes with groundwater, the gas compositions may be disturbed, e.g. by the addition of atmospheric air.

6. SUMMARY AND CONCLUSIONS

Several gas geothermometers have been applied to selected geothermal fields. The results for some of the gas geothermometers suggested by Arnorsson et al. (1985) are close to those expected. One reason is that these geothermometers were to a certain extent, calibrated using sample concentrations from the Icelandic fields. Whether they are applicable in other countries needs to be verified. The gas composition from fumaroles generally indicates higher temperatures than those measured in nearby wells, probably due to condensation during upflow. In theory, the more soluble the gas is, the less its concentration is affected by condensation. In low temperature fields, the CO_2 - temperature tends to be slightly lower than that of H_2S (see Figure 23). The removal of H_2S and H_2 from steam will indicate low subsurface temperatures for geothermometers based on the concentrations these gases. The best way is to use different gas geothermometers together and, thus, get more information from gas composition. Magmatic gases entering reservoirs will cause a high CO_2/H_2S ratio and high CO_2 - temperatures, but a relatively stable H_2S - temperature. The CO_2 - temperature will tend to recover gradually to its original state after magmatic activity has stopped.

The mineral buffers pyrite + magnetite + epidote + prehnite are suggested to control the H_2S concentration in the fluids of the Bakki, Hveragerdi, Haedarendi and the upper zone Krafla fields, where inflow temperature does not exceed $220^\circ C$. It ought to be verified in other low-temperature geothermal fields and it should be possible to propose new gas geothermometers based on this chemical reaction. For the high temperature range, the controlling buffers should probably be pyrite + pyrrhotite + epidote + prehnite. The mineral buffer zoisite + prehnite + calcite + quartz is likely to control the CO_2 concentration in reservoirs. But it is found to deviate from ideal curves, and mineral activity, which is difficult to determine, has to be taken into account.

In most cases, the Fischer-Tropsch reaction does not approach equilibrium in the reservoirs

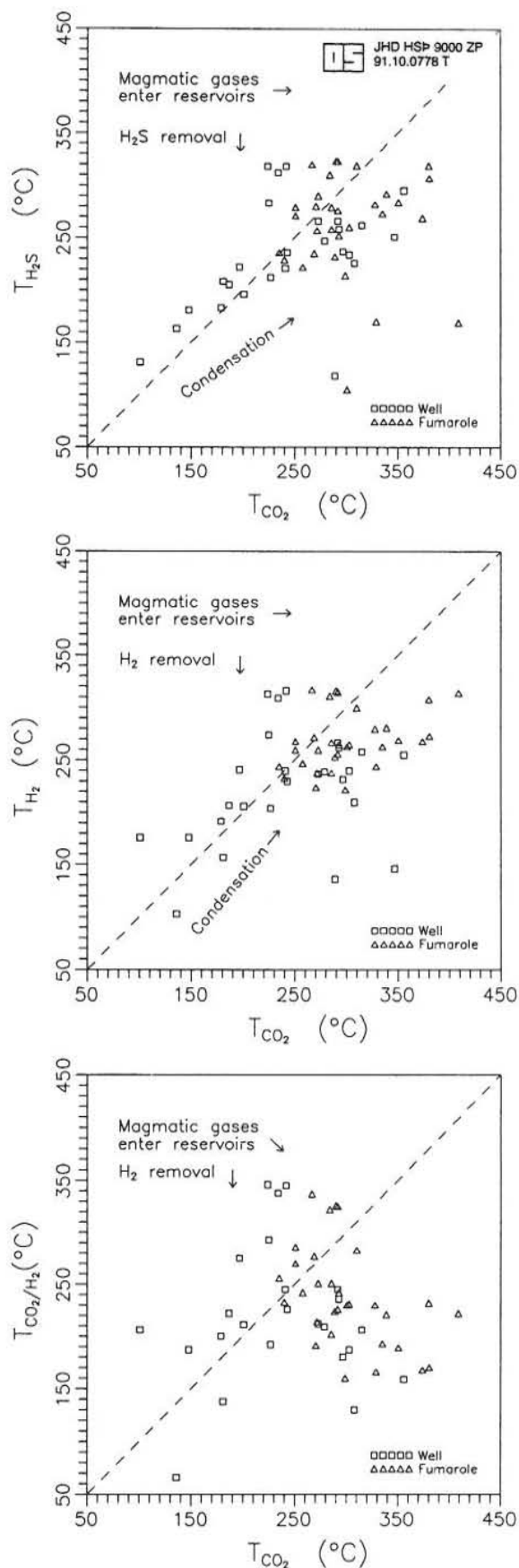


FIGURE 23: Comparison of the results of different gas geothermometers

studied, with the exception of the lower zone in the Krafla field. The method suggested by D'Amore and Truesdell (1985) is applied with success to inflow from that zone. The extensive boiling in boreholes may cause the composition of the discharge not to represent the composition of the original fluid in the reservoirs. The thermodynamic methods cannot be used in such a situation because their assumptions are not met.

Several gas geothermometers are not suited for Icelandic geothermal fields. The main reason is incorrect basic assumptions, such as that carbon dioxide is fixed by an external agent, that graphite takes part in chemical reactions and that the Fischer-Tropsch reaction is in equilibrium. It is necessary to evaluate the assumptions made before applying each gas geothermometer in a particular situation. Some gas geothermometers have been applied to certain geothermal fields with success, but they may be unsuitable for other geothermal fields due to different geological environments. Thermodynamic methods provide a useful way to understand the behaviour of geothermal fields, but correct assumptions must be made for practical studies.

ACKNOWLEDGEMENTS

I admire my advisor Dr. Halldor Armannsson, who is scrupulous and serious in his work, and would like to express my appreciation to him for his unselfish devotion and patient guidance. Special thanks to Dr. Ingvar Birgir Fridleifsson for his selection of candidates for the course and making elaborate arrangements. Ludvik S. Georgsson is thanked for his assistance and useful advice during the whole course. Prof. Stefan Arnorsson and Dr. Einar Gunnlaugsson are thanked for beneficial discussions. Thanks to Dr. Jon Orn Bjarnason for his good suggestions for my project; to Magnus Olafsson, for his directions on how to run the WATCH programme; to the staff of the chemical laboratory, for their help in analytical work; to Grimur Bjornsson, for his logging of Krafla well K26; to Marcia Kjartansson, for editing this report; to all the people who gave me help at Orkustofnun.

I also wish to thank Prof. Wang Jiyang for his recommendation to the Geothermal Training programme, the United Nations University, and to the Institute of Geology, the Chinese Academy of Sciences for permitting me to interrupt my Ph.D. programme for six months. Thanks to the Icelandic people for their kindness and hospitality. I will remember this marvellous period during which I stayed on the Atlantic Ridge.

REFERENCES

- Armansson, H., 1987: Studies on the geochemistry of steam in the Suswa and Longonot areas and water in the Lake Magadi, Kedong Valley and Lake Turkana areas, Rift Valley, Kenya. UNDTCD, Government of Kenya, technical report, 54 pp.
- Armansson, H., and Gislason, G., 1991: Krafla - KG-25. Start of discharge and production test. Flow-chemical properties of fluid. Orkustofnun, Iceland, report OS-91023/JHD-10 B (in Icelandic), 37 pp.
- Armansson, H., Benjaminsson, J., and Jeffrey A.W.A., 1989: Gas changes in the Krafla geothermal system, Iceland. *Chem. Geol.*, 76, 175-196.
- Armansson, H., Gislason, G., and Torfason, H., 1986: Surface exploration of the Theistareykir high-temperature geothermal area, Iceland, with special reference to the application of geochemical methods. *Appl. Geochem.*, 1, 47-64.
- Armansson, H., Gudmundsson, A., and Steingrímsson, B.S., 1987: Exploration and development of the Krafla geothermal area. *Jokull*, 37, 13-29.
- Arnorsson, S., 1986: Chemistry of gases associated with geothermal activity and volcanism in Iceland - a review. *J. Geophys. Res.*, 91, 12.262-12.268.
- Arnorsson, S., 1987: Gas chemistry of the Krisuvik geothermal field, Iceland, with special reference to evaluation of steam condensation in upflow zones. *Jokull*, 37, 31-49.
- Arnorsson, S., 1990: Gas chemistry of geothermal systems. Geochemistry of gaseous elements and compounds. In: (Ed.) Durrance, E.M., et al. Theophrastus publications, S.A., 187-222.
- Arnorsson, S., and Gunnlaugsson, E., 1985: New gas geothermometers for geothermal exploration - calibration and application. *Geochim. Cosmochim. Acta*, 49, 1307-1325.
- Arnorsson, S., Sigurdsson, S., and Svavarsson, H., 1982: The chemistry of geothermal waters in Iceland. I. Calculation of aqueous speciation from 0° to 370°C. *Geochim. Cosmochim. Acta*, 46, 1513-1532.
- Arnorsson, S., Sigurdsson, S., and Svavarsson, H., 1983a: The chemistry of geothermal waters in Iceland II. Mineral equilibria and independent variables controlling water compositions. *Geochim. Cosmochim. Acta*, 47, 547-566.
- Arnorsson, S., Sigurdsson, S. and Svavarsson, H. 1983b: The chemistry of geothermal waters in Iceland III. Chemical geothermometry in geothermal investigations. *Geochim. Cosmochim. Acta*, 47, 567-577.
- Barnes, I., Irwin, W.P., and White, D.E., 1978: Global distribution of carbon dioxide discharges and major zones of seismicity. U.S. Geol. Surv., Water-Resources Investigations, 78-39, 12 pp.
- Benjaminsson, J., and Hauksson, T., 1990: The Krafla area. Studies on fumaroles 1990. Landsvirkjun, Iceland, report (in Icelandic), 43 pp.
- Berman, R.G., 1988: Internally-consistent thermodynamic data for minerals in the system Na_2O -

- $K_2O-CaO-MgO-FeO-Fe_2O_3-Al_2O_3-SiO_2-TiO_2-H_2O-CO_2$. *J. Petrol.*, 29, 445-522.
- Bjornsson, A., 1985: Dynamics of crustal rifting in NE Iceland. *J. Geophys. Res.*, 20, 1515-1530.
- Bottinga, Y., 1969: Calculated fractionation factors for carbon and hydrogen isotope exchanges in the system calcite-carbon dioxide-graphite-methane-hydrogen-water vapour. *Geochim. Cosmochim. Acta*, 33, 49-64.
- Craig, H., 1975: Isotopic temperatures in geothermal systems. Presented at the I.E.E.A. Advisory Group on the Application of Nuclear Techniques to Geothermal Studies, Pisa.
- D'Amore, F., and Nuti, S., 1977: Notes of chemistry of geothermal gases. *Geothermics*, 6, 39-45.
- D'Amore, F., and Panichi, C., 1980: Evaluation of deep temperatures in geothermal systems by a new gas geothermometer. *Geochim. Cosmochim. Acta.*, 44, 549-556.
- D'Amore, F., and Truesdell, A.H., 1985: Calculation of geothermal reservoir temperatures and steam fractions from gas compositions. *Trans. Geoth. Res. Council*, vol. 9-1, 305-310.
- D'Amore, F., and Truesdell, A.H., 1988: A review of solubilities and equilibrium constants for gaseous species of geothermal interest. *Sci. Geol. Bull.*, 41, 309-332.
- D'Amore, F., Celati, R., and Calore, C., 1982: Fluid geochemistry applications in reservoir engineering (vapor-dominated systems), Proc., 8th Workshop Geothermal Reservoir Engineering, Stanford, 296-307.
- D'Amore, F., Fancelli, R., Saracco, L., and Truesdell, A.H., 1987: Gas geothermometry based on CO content. Application in Italian geothermal fields. Proc. 12th Workshop Geothermal Reservoir Engineering, Stanford, 247-252.
- Darling, W.G., and Armannsson, H., 1989: Stable isotopic aspects of fluid flow in the Krafla, Namafjall and Theistareykir geothermal systems of Northeast Iceland. *Chemi. Geol.*, 76, 197-213.
- Ellis, A.J., 1957: Chemical equilibrium in magmatic gas. *Am. J. Sci.*, 255, 416-431.
- Giggenbach, W.F., 1980: Geothermal gas equilibria. *Geochim. Cosmochim. Acta*, 44, 2021-2032.
- Giggenbach, W.F., 1981: Geothermal mineral equilibria. *Geochim. Cosmochim. Acta*, 45, 393-410.
- Hauksson, T., and Benjaminsson, J., 1990: The Krafla Power Station. Flow and chemical composition of water and steam in boreholes and production apparatus in May 1990. *Landsvirkjun - Krafla Power Station, Iceland*, report (in Icelandic), 56 pp.
- Helgeson, H.C., 1969: Thermodynamics of hydrothermal systems at elevated temperatures and pressures. *Amer. J. Sci.*, 267, 729-804.
- Helgeson, H.C., and Kirkham, D.K., 1974: Theoretical prediction of the thermodynamic behavior of aqueous electrolytes at high pressures and temperatures. *Amer. J. Sci.*, 274, 1890-1261.
- Helgeson, H.C., Delany J.M., Nesbitt, H.W., and Bird, D.K., 1978: Summary and critique of the thermodynamic properties of rock forming minerals. *Amer. J. Sci.*, 278A, 1-229.

Kacandes, G.H., and Grandstaff, D.E., 1989: Differences between geothermal and experimentally derived fluids: How well do hydrothermal experiments model the composition of geothermal reservoir fluid? *Geochim. Cosmochim. Acta*, 53, 343-358.

Muna, Z.W., 1982: Chemistry of well discharges in the Olkaria geothermal field, Kenya. UNU G.T.P., Iceland, report 8, 38 pp.

Nehring, N.L., and D'Amore, F., 1984: Gas chemistry of the Cerro Prieto, Mexico, geothermal field. *Geothermics*, 13, 75-89.

Olafsson, M., 1988: Sampling methods for geothermal fluids and gases. Orkustofnun, Iceland, OS-88041/JHD-06, 17 pp.

Oskarsson, N., 1984: Monitoring of fumarole discharge during the 1975-1982 rifting in Krafla volcanic center, North Iceland. *J. Volc. Geoth. Res.*, 22, 97-212.

Tonani, F., 1973: Equilibria that control the hydrogen content of geothermal gases. Philips Petroleum Co., unpublished report (reported in: Carapezza, M., Nuccio, P.M., and Valenza, M., 1980. *Bull. Volcanol.*, 44, 547-564).

Tonani, F. 1980: Some remarks on the application of geochemical techniques in geothermal exploration. *Proc. 2nd Int. Res. E.C. Geothermal En. Research*, 428-443.

Truesdell A.H., and Nehring, N.L. 1978/1979: Gases and water isotopes in a geochemical section across the Larderello, Italy, geothermal field. *Pageoph.*, 117, 276-289.